3-9-2011

Rheological characteristics of solvent free nanofluids: Thermal transitions and reactive curing

Daniel Chojnowski
Eastern Michigan University

Rheological Characteristics of Solvent-Free Nanofluids: Thermal Transitions and Reactive Curing

Daniel Chojnowski

Thesis

Submitted to the School of Engineering Technology

Eastern Michigan University

in partial fulfillment of the requirements

for the degree of

MASTER OF SCIENCE

in

Polymer and Coating Technology

Thesis Committee:

John Texter, PhD, Chair

Wade Shen, PhD

Vijay Mannari, PhD

March, 2011

Ypsilanti, MI

THESIS APPROVAL FORM

Rheological Characteristics of Solvent Free Nanofluids: Thermal Transitions and Reactive Curing

Daniel Chojnowski

ACKNOWLEDGEMENTS

I would like to thank Prof. John Texter for his support and guidance throughout this project. Second, I would like to thank Zhiming Qiu, and Kejian Bian, for providing the analyzed solvent free nanofluids. Last, I would also like to thank my wife for her continued support and patience, and father-in-law for his continued lack of patience.

ABSTRACT

Solvent-free nanofluids are a new and exciting class of material that evolved to address the limitations of their predecessors, nanocomposites. One of the most exciting aspects of solvent-free nanofluids is the wide range of tools chemists have to build and study them. Understanding how the structure manipulations impact the rheology of the resulting solvent-free nanofluids is essential if solvent-free nanofluids are truly the technology of the future. This work documents the basic rheological parameters, thermal transitions, and curing kinetics of various solvent-free nanofluids synthesized by Zhiming Qiu and Kejian Bian at the Coating Research Institute at Eastern Michigan University.

TABLE OF CONTENTS

LIST OF TABLES

LIST OF FIGURES

Figure Page

Chapter 1

Introduction to Rheology

Rheology can be defined as the study of a material's deformation under an applied stress.[1] Over time, rheology has evolved into a science of its own. Most rheology discussions revolve around the rheology of a specific material or class of materials. As with any science, a fundamental understanding of the "language" associated with the science must be understood before applying it or engaging in the conversation

Perhaps the most common term associated with rheology is viscosity. In layman's terms, viscosity can be defined as a material's thickness. In mathematical terms, viscosity is defined as $\eta=\tau/\gamma$, where η is the viscosity, τ is the shear stress and γ is the shear rate. In other words, viscosity can be thought of as a fluid's resistance to deformation when a stress is applied. [1] Viscosity can be classified further as either kinematic or dynamic viscosity. Kinematic viscosity is the dynamic viscosity divided by the material density.[1] For some types of viscosity measurements (like in a falling ball viscometer) the kinematic viscosity is what is measured directly. A separate density measurement would be needed to get the dynamic viscosity. For other measuring devices (like the TA Instrument's AR-G2 I used in this work), the dynamic viscosity is what is measured directly; a separate density measurement would be needed to get the kinematic viscosity.

How the viscosity is affected by applying shear stress is what classifies the material into one of three generic classes. The first class is Newtonian fluids. Materials that are Newtonian exhibit a linear response to shear stress with increasing shear rate.

Recall that viscosity is defined as shear stress divided by shear rate. Newtonian liquids do not exhibit a viscosity change with increasing or decreasing shear stress. Perhaps the most common example of a Newtonian fluid is water.[1]

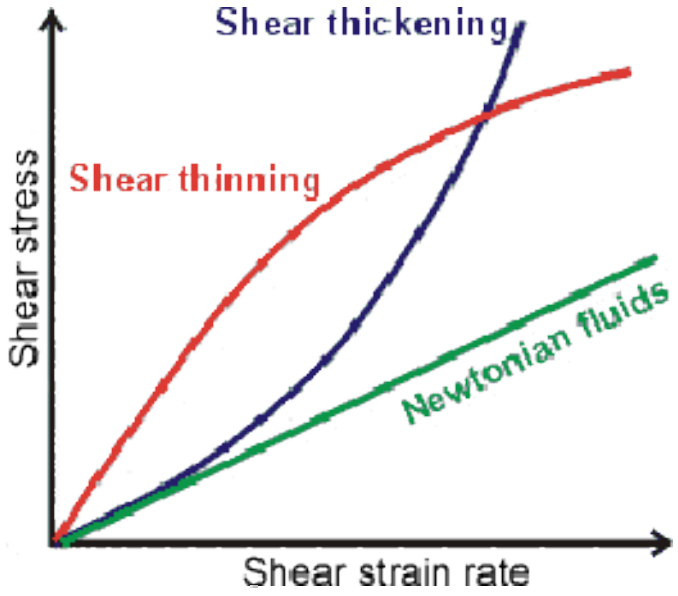

Figure 1-1. Newtonian, shear thinning, and shear thickening fluids.

The second most common material classification is shear-thinning fluids (also referred to as pseudoplastici fluids). Shear thinning fluids exhibit a decrease in viscosity with increasing shear stress.[2] Common types of shear thinning fluids include polymer solutions, paints, ketchup, colloidal dispersions and whipped cream.[2] Typically, shear thinning fluids contain a measurable degree of internal structure that arises from interactions between different components or attractive forces within the material. When a force capable of disrupting the internal structure is applied to the structured fluid, the material begins to yield or shear thin.[1]

The third and least common classification is shear thickening (also referred to as dilatant). As the name suggests, fluids that are shear thickening increase in viscosity when shear is applied. The dilatant effect occurs when closely packed particles are combined with enough liquid to fill the gaps between them. At low velocities, the liquid acts as a lubricant, and the dilatant flows easily. At higher velocities, the liquid is unable to fill the gaps created between particles, and friction greatly increases, causing an increase in viscosity.[1] An easy-to-construct illustration of this effect can be seen with a mixture of cornstarch and water.

In addition to these three main classes, thixotropic fluids exist as a subclass of shear thinning fluids. Thixotropic fluids decrease in viscosity over time while under constant shear.[2] Unfortunately, the term *thixotropic* is common used interchangeably with shear thinning. Almost all thixotropic fluids are also shear thinning, but the inverse is not necessarily true.

Viscoelasticity is another fundamental term in rheology. *Viscoelasticity* is the term used to describe materials that exhibit both viscous and elastic responses when undergoing deformation[1] Viscous materials are those that resist deformation when a stress or strain is applied. Elastic materials are those that deform immediately but return to their original shape, after the deforming stress is removed. Most materials exhibit a combination of viscous and elastic responses under stress or deformation.[2] Robert Hooke developed his theory of elasticity. "The power of any spring is in the same proportion with the tension thereof."[3] Meanwhile Isaac Newton, addressed liquids and steady shearing flow in *Principia*.[3] "The resistance which arises from the lack of slipperiness of the parts of the liquid, other things being equal, is proportional to the

velocity with which the parts of the liquid are separated from one another."[3] Materials behave in the linear manner, as described by Hooke and Newton, only on a small scale in stress or deformation.[3] Viscoelastic materials have elements of both of these properties and, as such, exhibit time dependent strain. Whereas elasticity is usually the result of bond stretching along crystallographic planes in an ordered solid, viscosity is the result of the diffusion of atoms or molecules inside an amorphous material.[3]

Perhaps as important as viscosity are the terms *storage* and *loss moduli*. The storage modulus is a quantity that express how much energy the material is capable of storing.[4] Conversely, the loss modulus is a quantity that describes how much energy the material inelastically loses or dissipates. Both of these quantities are measured during oscillatory rheology.[4] A classical and easy to comprehend example of the storage and loss modulus can be described by imagining a dropping ball from some height x. The height (y)(m)(g), at which the ball bounces back up can be thought of as the storage modulus. The loss modulus would be represented by (x-y)(m)(g).

Additionally, it is often useful to view the relationship of the storage and loss modulus as a quotient referred to as tan delta. Tan delta is the quotient of the loss moduli / storage moduli.[1] The tan delta parameter is popular because it is directly related to the energy lost per cycle divided by the energy stored per cycle. Observing changes in the tan delta is a useful means of evaluating the transition from liquid-like to solid-like behavior. It describes the energy-damping behavior of a material.[2] In addition, it often affords insight into the loss spectrum (as a function of frequency) that might not be evident from examining the loss and storage moduli alone.[2]

Understanding the preceding should provide a solid foundation that can be built upon. With that background it is possible to begin to explore how rheometers operate and then focus on the rheology of some commonly analyzed systems.

The manner in which scientists explore a material's rheology has, like most sciences, evolved considerably over the last few decades. Modern rheometers will measure or control three variables: torque, angular displacement, and angular velocity. The first parameter, torque, is described as the measure of how much force acting on an object causes that object to rotate. In mathematical terms, the amount of torque is defined as $M = r*F \sin(\theta)$, where M is torque, F is force, and r is the distance from the pivot to the point of where the force acts. During the vast majority of rheological measurements, torque is applied in a rotational format. The mathematical expression in this case is defined as $M = I \alpha$, where α is the angular acceleration, and I is the moment of inertia. The rheometer utilizes the measured torque to calculate the stress applied to the sample. The equation utilized to calculate the stress is defined as $s = K_s M$, where s is stress, M is torque, and K_s is a stress constant that is assigned depending on the chosen geometry. The torque is proportional to stress as it is related through the geometry constant. The rheometer's torque range is fixed, but the stress range is variable as it depends on what type and size of geometry selected. This enables the rheologist to control the desired stress level.

The second parameter that is measured or controlled is the angular displacement. Angular displacement is the angle or distance that a rotating body goes through. Modern day rheometers have the capability of performing both tasks by measuring the displacement using an optical encoder.[1]

The last parameter is the angular velocity. The angular velocity is measured under application of torque. From the angular velocity is it now possible to calculate the shear rate. The equation utilized to express shear rate is $\gamma = K_\gamma \times \Omega$, where γ is shear stress, K_γ is a strain constant that is specific to the chosen geometry, and Ω is the applied angular velocity. Relating the information discussed above it is now possible to derive how modern rheometers measure viscosity.

A wide variety of oscillatory measurements are possible with modern day rheometers. In almost all cases, multiple measurements are necessary to truly explore a material's rheology. Furthermore, it is often the case that many preliminary experiments are conducted to determine the proper acquisition parameters prior to conducting the experiment of interest. The following is a quick highlight of the most common oscillatory measurements.

Stress sweep is an extremely common oscillatory experiment. A stress sweep simply does what it implies. The analyst identifies the frequency and temperature, and the instrument varies the amount of stress applied to the sample. A very similar experiment is strain sweep, which varies the amount of strain over a predetermined interval. Plotting the stress as the x-axis and storage and loss modulus as the y-axis, the effect of stress can easily be assessed.

Frequency sweep is another extremely common oscillatory experiment. The temperature and stress are defined, and the instrument varies the frequency in which the stress is applied. Plotting the frequency as the x-axis and storage and loss modulus as the y-axis makes it vary to assess the effect of frequency.

While conducting measurements, it is extremely important that the measurements are done within the linear viscoelastic range (LVR).[4] The LVR can be thought of as the combination of temperature, stress, and frequency that can be applied to a sample without disrupting the internal structure of the sample. When measurements are taken while a sample's internal structure is already disrupted, it is easy to understand that the collected data are not reliable (when represented as linear measurements).[5] However, when data are presented without justification or proof that the LVR was adhered to, it is impossible for the reader to have confidence in the data's reliability. To determine what combination of parameters fall within the LVR, a stress sweep is normally first conducted using the desired frequency and temperature. The LVR can be assessed by plotting stress along the x-axis and the storage and loss modulus along the y-axis, and then looking for the stress range where the storage and loss modulus run parallel with each other and the x-axis. It should be noted that the newly defined LVR is specific to the chosen temperature and frequency. If the analyst plans on conducting experiments at multiple temperatures or frequencies, the LVR will again have to be determined. Another manner for visualizing the LVR is described from Bill Grassley of Princeton University.

> If the deformation is small, or applied sufficiently slowly, the molecular arrangements are never far from equilibrium. The mechanical response is then just a reflection of dynamic processes at the molecular level which go on constantly, even for a system at equilibrium. This is the domain of liner viscoelasticity. The magnitudes of stress and strain are related linearly, and the behavior for any liquid is completely described by a single function of time.[6]

After the LVR range has been identified, the next step in method development is to verify the sample is stable. The stability is judged by conducting a time sweep.[5] Any combination of frequency, stress, and temperature that fell within the LVR can be utilized

as the acquisition parameters. The time sweep is simply going to analyze the sample under the described conditions for a specific length of time (ten minutes is the unwritten, universal standard). Once the test has concluded, plotting the storage and loss modulus as the y-axis against time as the x-axis will allow for a quick determination whether the sample is stable. The sample is said to be stable if the storage and loss modulus are again parallel to each other and the x-axis. If the sample is not stable, its stability needs to be addressed. If the experimenter believes the in-stability is attributed to the test conditions such as exposure to oxygen or atmospheric moisture, accessories that utilize nitrogen purges or apparatuses that prevent solvent from escaping are readily available.

A temperature sweep is an experiment that attempts to gauge the effect of temperature on the sample. During a temperature sweep, the stress and frequency are defined and the instrument incrementally increases the temperature. It is important to note that the instrument step-wise increases the temperature, and typically an equilibration time is given at each temperature interval.[5]

A temperature ramp is extremely similar to a temperature sweep, but this time the instrument linearly increases the temperature and measures the rheology without equilibration.[5]

The background provided up to this point should now be adequate to serve as a foundation when discussing the rheology of specific systems. The usefulness of rheology arises from creating relationships from the materials structure and the resultant rheological properties. For that reason the common rheological properties of polymer melts, colloidal dispersions, and emulsions will be discussed.

Polymer melts are a nice example of how the molecular structure directly influences the rheological properties of the melt. Polymer melts are polymers that have been heated past their melting point. They are generally non-Newtonian fluids, and the vast majority are shear thinning. The fundamental aspects of polymer rheology directly relate to the manner in which polymeric chains interact with one another. This interaction is the result of molecular weight, molecular weight distribution, and attractive forces.[7] The first rheological property of polymer melts of interest is the viscosity of polymers at low shear rate. Typically the low shear rate viscosity is linear and is often referred to as the zero shear viscosity or the viscosity of the first Newtonian plateau. An illustration of a polymer flow curve is shown in Figure 1-2.[5] This viscosity is of high interest when it comes to polymer melts, as the zero shear viscosity often has a high influence on the final appearance of the final product. The viscosity of polymer melts at moderate shear rates is shear thinning. The stress at which the material begins to shear can be attributed to the molecular weight or, for constant molecular weight, can be associated with polydispersity. Given two polymer melts of equivalent weight average molecular weights the polymer with the higher polydispersity will shear at lower stresses.[8] This is important in processing polymer melts, as the lower the viscosity, the less shear that needs to be put into the system. In regard to branched polymers, the degree of branching, length of the branching, and the actual location of the branching relative to the back bone has an influence on the melt's rheology.[9] Increasing the number, the size, or the flexibility of the branches changes the melt viscosity. For example, if the branches are few and long enough to entangle, melt viscosity will be higher at low frequency than that of a corresponding linear polymer of the same

molecular weight. Additionally the viscosity of long branched polymers is more shear rate dependant than the viscosity of linear polymers.[10] The use of rheology to optimize the process parameters of polymer melts is a powerful and insightful tool.

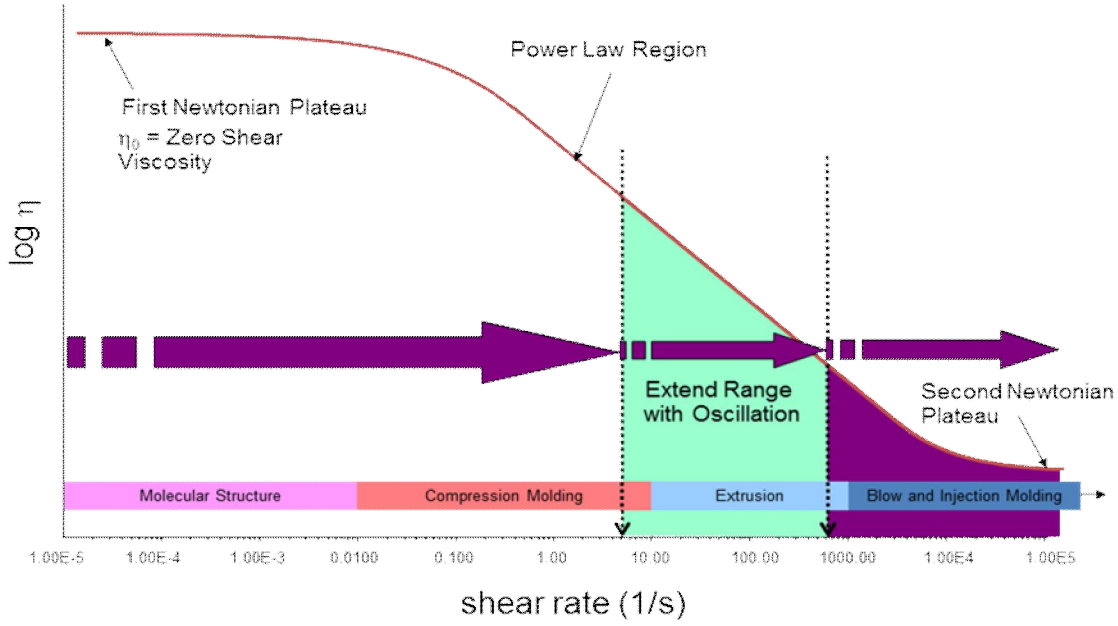

Figure 1-2. Illustration of a polymer melt's typical flow curve.[5]

The rheology of colloidal dispersions has some similarities to polymer rheology; after all they are both structured fluids.[4] The formation of the internal structure is, however, drastically different. The internal structure of colloidal dispersions arises from the interaction of the dispersed solid particles.[11] The volume fraction of the dispersed colloids has large implications on the systems rheology. Furthermore, given the large surface area to volume ratio of colloids, the surface chemistry is also important. To complicate matters further, the size range of colloids has a significant influence on the

dispersion's rheology.[11] To truly study a dispersion's rheology the effect of colloidal size range, surface chemistry, Brownian forces, direct inter-particle forces, and viscous hydrodynamic consideration would need to be considered.[11] The phrase *viscous hydrodynamic consideration* is meant to describe the disturbance that a solid particle has on the suspending medium.[11] Under static conditions, the effective range of the above described influences are small.[4] The phenomenon that governs the rheology is how the particles rearrange to accommodate shear when it is applied. At low values of shear, the microstructure is simply pushed or carried away by the flow, and the resulting viscosity remains constant.[4] At increasing shear values, a yield stress is reached that begins to break apart the microstructure and orient the particles in the direction of the flow. As the shear increases, the viscosity returns to another Newtonian plateau. At increasingly higher shear rates it is possible that the particles can be forced together. The joining of particles creates a large object moving through the suspending medium. The larger object in turn creates a larger hydrodynamic effect, and the viscosity may then increase.[11] It should be mentioned that the joining of particles under strong shear is highly system specific.

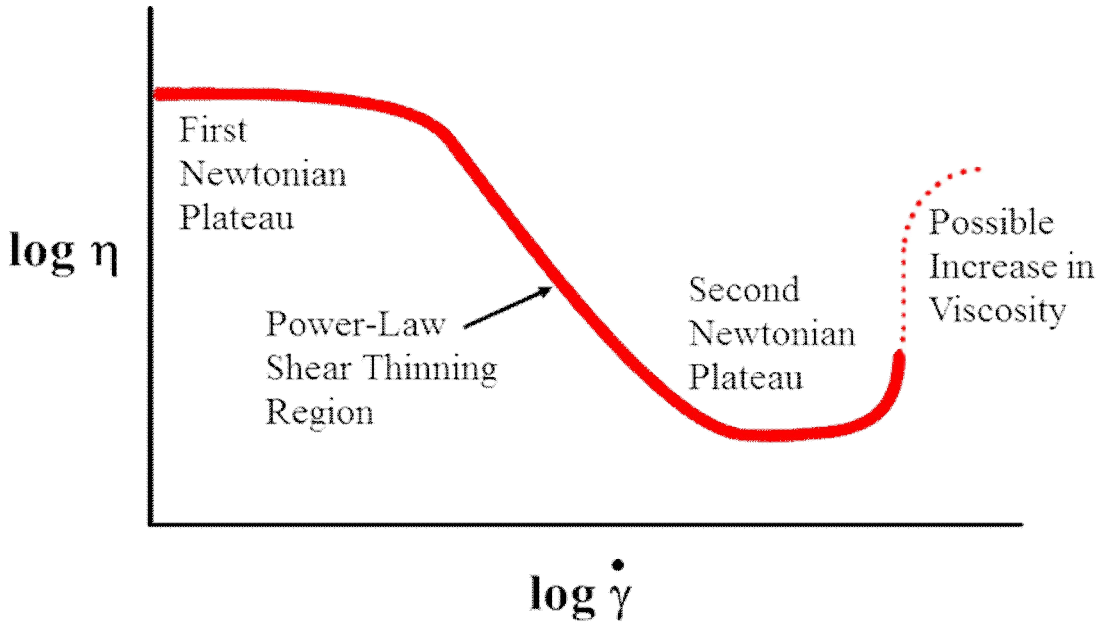

Figure 1-3. Illustration of typical colloidal dispersion's flow curve.[4]

In summary, the internal structure that arises from colloidal dispersions contains many variables of relatively equal importance, and thus directly relating rheological properties to anyone variable is extremely difficult. The manner in which the resulting microstructure forms and behaves under shear is relatively complex due to the high number of variables. However, controlling or predicting this complex behavior is of high interest to material scientists, chemists, physicists, and rheologists.[12,13]

Last, we discuss the rheology of emulsions. Emulsions are defined as dispersions of liquid droplets in a liquid suspending medium.[14] The rheological aspects discussed include viscosity of dilute emulsions, behavior of concentrated emulsions, deformation and break-up of droplets in emulsions during flow, blends of polymer melts as emulsions, and the role of surfactants in respect to stability and aging.

The viscosity of dilute emulsions increases linearly with increasing droplet concentration.[14] The point at which the viscosity no longer increases linearly is the point at which the emulsion is no longer classified as dilute. In dilute emulsions, the droplets have no interaction with each other. Assuming the medium in which the droplets are suspended is Newtonian itself, the dilute emulsion will also be Newtonian.[14]

The viscosity of concentrated emulsions is more noteworthy than that of dilute emulsions. After all, in most cases the dispersed phase is what is being delivered, and the continuous phase is just the delivery. The spectrum of concentrated emulsions begins where dilute emulsions stop, and ends at the point that no additional suspended droplets can be added without deforming the droplets that are already present.[14] As the concentration of the dispersed droplets increases, so does the zero shear viscosity. The behavior under shear is increasingly shear thinning as the concentration increases, much like colloidal dispersions. The extent of the shear thinning and yield point is dependent on the insoluble surfactant, the extent of deformation, and the deformations effect on the hydrodynamic volume of the dispersing phase.[15] When the droplet concentration begins to approach the limit of close packing, the interfacial layers' interaction can translate in a drastic build-up of internal structure. When this happens and shear is applied, shear thinning behavior can be extremely sudden.[14]

At a given stress, liquid droplets within a suspending medium will deform into an ellipsoid. At higher stress, the droplets will begin to break. The force that is resisting the deformation and breakup is the interfacial stress, as well as the viscosity of the continuous phase. The stress levels that are needed to create both the deformation and breakup are contingent upon the droplets' viscosity, continuous phase viscosity, and the

interfacial tension. This is one of the fundamental reasons that the viscosity of emulsions differs from that of colloidal dispersions.[14]

As previously mentioned, surfactants are important aspects in the rheology of emulsions. Although emulsions are thought of as having two phases, with respect to rheology it may be more accurate to think of them as three phase systems.[14] The molecular weight, amount of surfactant, and the hydrophilic / lipophilic balance governs the rheological properties of emulsions.[14] The surfactant is directly related to the manner in which the droplets interact at rest and deform under shear. It prevents aggregation at rest and is directly related to the storage stability. Utilizing rheology and examining the storage modulus over time with respect to different frequencies is a very effective means for analyzing stability.[14] Additionally, utilizing heat aging and then examining the rheology of the emulsion is an effective means for optimizing the surfactant choice.

Chapter 2

Introduction to Solvent-Free Nanofluids (SFNs)

Solvent-free nanofluids (SFNs) are a new and exciting class of materials that evolved to address the limitations of their predecessors, nanocomposites.[16] Nanocomposites are essentially nanoparticles dispersed in a polymer or other solid matrix.[17] Dispersing nanoparticles in a polymer matrix can effectively improve the properties of the dispersing polymer and bring a new set of unique properties to the matrix.[16] Nanocomposites have generated a lot of industrial attention and are predicted to grow 24% in 2011 to reach a usage of 45 million kilograms ($500 – 800 million).[16] The limitations surrounding nanocomposites are their poor miscibility, dispersion, and interfacial strength. SFNs most often are organic-inorganic hybrid materials that consist of a nanoparticle core functionalized with a covalently bonded, positively charged, aliphatic chain.[16,18] An anionic counter ion is also present to balance the charge. This particular configuration gives SFNs, as an entire class of materials, a unique set of properties. The vast majority of metals, especially transition metals, require heat in excess of 1000 ^{0}C to flow as a liquid. Simply put, the amount of heat required drastically limits the usage and transportation of such metals. Converting these metals, which meets specific criteria discussed below, into SFNs allows these metals to exhibit liquid-like properties at room temperature in the absence of solvent.[18] It is the absence of solvent that distinguishes this class of materials from traditional colloid suspensions.[16] In additional SFNs also exhibit zero vapor pressure.[18,19] Potential uses for SFNs include alternative coolants for several thermal management applications, including transportations, MEMS, microelectronics and refrigeration systems.[18] Significant

increases in thermal conductivity have been reported even at low fractions of nanoparticles.[19] The small size of SFNs as constituent particles may find uses as lubricants designed to reduce the wear in solid-solid contacts.[18] It is also possible that SFNs may alleviate the environmental concern with traditional nanoparticles. This approach brings about an effective means to incorporate nanoparticles into films and coatings. SFNs also have potential to offer solvent-free conducting fluids, and magnetic or electrorheological fluids. Last, the dimensions of nanoparticles along with their intrinsic physicochemical properties may lead SFNs to find multiple uses as reaction media.[19]

The initial approach for generating SFNs has been to graft a charged oligomeric chain on a nanoparticle core. When this initial process is completed, a counter anion, typically chlorine, is present to balance the charge. The hard chloride anion is then replaced with a soft sulfonate anion, and the resulting material is a SFNs. At this point, before expanding on the generalized approach described above, it is useful to identify and define some terms that have become common language to SFNs researchers.[16] The first term is the core. The core is the center of SFNs, composed entirely of the chosen nanoparticle. The second term is the corona; the corona is the positively charge aliphatic chain covalently boned to the surface of the core. Last is the canopy; the canopy is the combination of both the corona and the counter ion.

An example of this type of synthesis would start with selecting a nanoparticle core with hydroxyl groups on the surface such as silica and reacting the hydroxyl groups with a $(CH_3O)_3Si(CH_2)_3N^+(CH_3)(C_{10}H_{21})Cl^-$. At this point, when Cl^- is the counter anion, the corona is a solid powder at room temperature that decomposes before melting.

However, when the Cl^- is exchanged with a soft sulfonate anion such as ($C_{13}H_{27}(OCH_2CH_2)_7O(CH_2)_3SO_3^-$), a SFNs is created that exhibits liquid like properties at room temperature. The reaction mechanism is shown below in Figure 2-1.

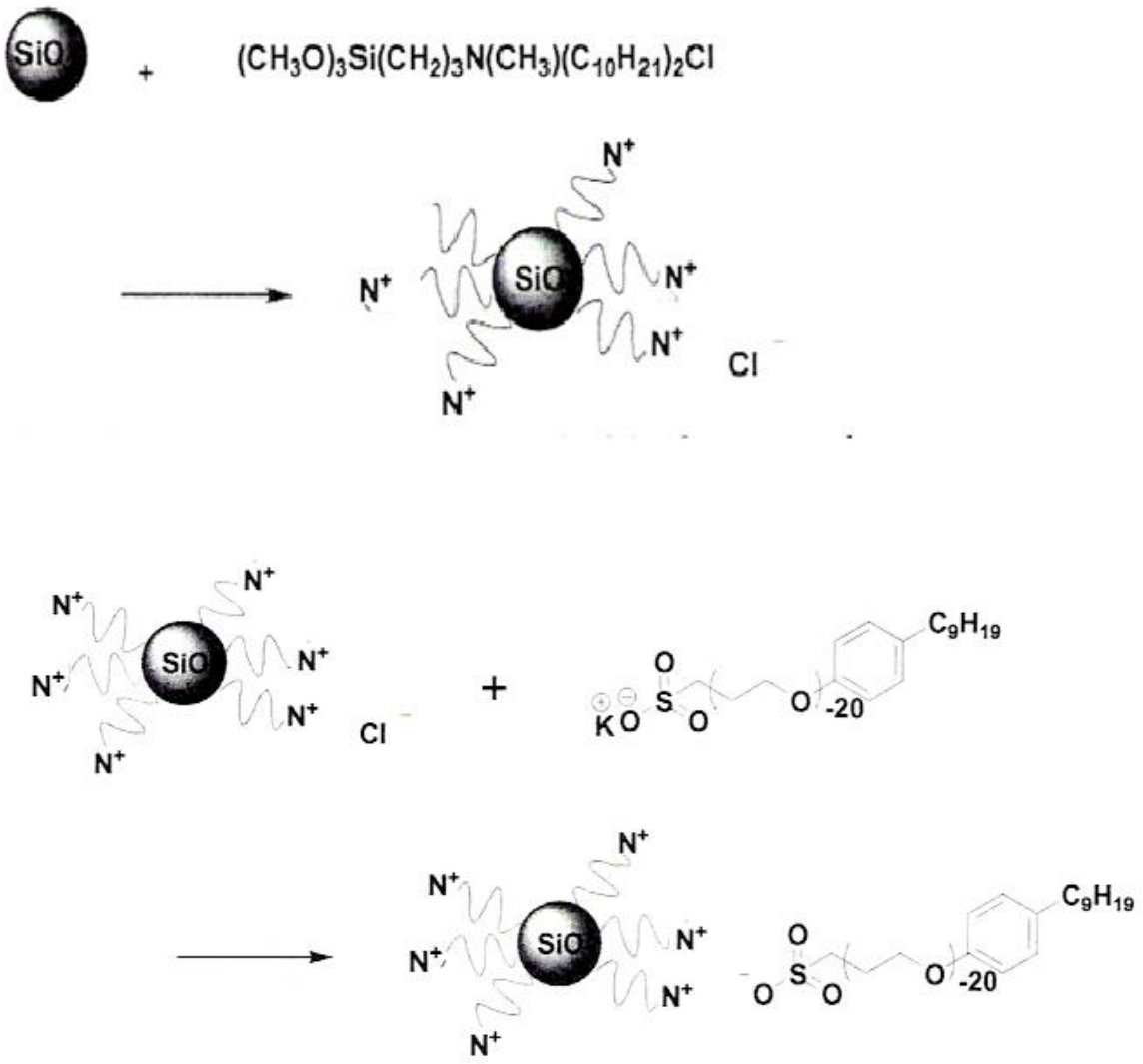

Figure 2-1. Illustration of first generation SFNs synthesis.

An additional approach or a "second generation" approach has also been developed in creating SFNs. The advantage of this approach when contrasted against the first approach is the ability to create large industrial quantities of SFNs. The first step of

this approach is to functionalize the oxide nanoparticle core. At this point in the process, the material is negatively charged and a proton is present to neutralize the species. Reacting this material which is effectively behaving as a strong acid with a tertiary amine or weak base results in an amber colored molten salt. A representative process is shown in the Figure 2-2[16].

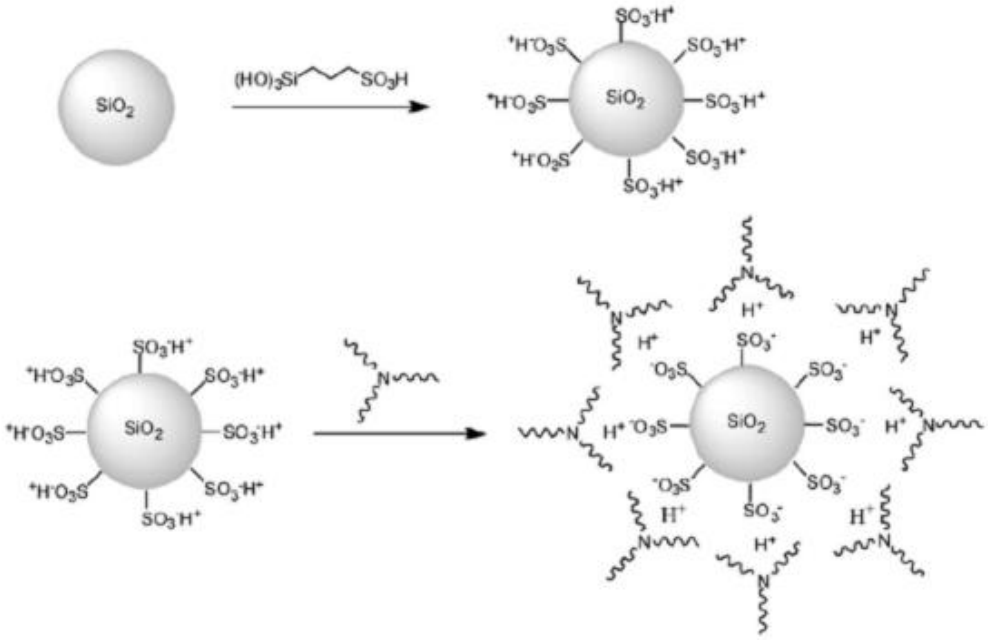

Figure 2-2. Illustration of second generation SFNs synthesis.[16]

First the nanoparticles are surface functionalized by condensation with a sulfonate organosilane to form the corona. Secondly, the acidic particles are neutralized with the tertiary amine (which serves as the canopy) in an acid-base reaction.[16]

SFNs deviate from both nanocomposites and colloidal suspensions in at least three different ways. The first is that the covalently bonded corona and counter ion serve

as the suspending medium for the nanoparticle core. The second is that the hybrid nature of the core and canopy imparts an extremely large formulation window. It is possible to imagine a single corona chemistry used to create an entire family of stable materials. The last is the covalently attached corona and screened electrostatic charge that stabilizes the SFNs core particles.[16]

The exact reason for the liquid-like behavior is still not completely understood, but a leading explanation has seemed to emerge in the literature. There is no doubt that the highly organic content of the material, nanometer size, and density of the nanoparticle all play a role in generating the liquid characteristics.[18] It is also believed that the bulky and highly asymmetric nature of the organic anions leads to a very frustrated molecular packing.[19] It may likely be a combination of all the discussed factors that gives SFNs its novel properties.

SFNs can be formulated to span the spectrum of glassy solids to nano-ionic liquids by manipulating the core particle, volume fraction of the core particle, canopy, canopy grafting density, varying the molecular weight of the canopy, and the counter ion species. The rheology of SFNs is an often discussed topic when a new SFNs' structure is presented in the literature.[19] Manipulating the previously mentioned variables has the capability to generate extremely complex rheological behavior to simple Newtonian flow behavior. There has also been research to suggest that the bulky anions appear to control the glass transition temperature of the system, viscoelastic properties, and the control of the local mobility.[20] It should be noted, however, that although the research indicates the counter ion influences the above mentioned properties, no theoretical explanation is available.

In summary, the manner in which SFNs are constructed affords the designer a large degree of synthesis options. This results in enhanced formulation flexibility when compared to nanocomposites and colloidal suspensions. The nanoparticle core of SFNs is stabilized utilizing the covalently bonded corona and electro-statically held counter anion.[20] This stabilization mechanism results in a material with liquid-like properties at room temperature in the absence of solvent and a material that has zero vapor pressure. The list of potential applications of this material is vast due to the flexibility in design.[20]

Chapter 3

Introduction to Ionic liquids

Ionic liquids (ILs) are salts that melt at or below 100 °C. Chloroaluminates were the first generation of ILs developed in 1950s; however, their application was limited because of moisture and air sensitivity. In 1992 an air-stable ionic liquid was reported, and since that time the ILs research has drastically expanded.[21] Ionic liquids typically consist of quaternary ammonium cations such as imidazolium, pyridinium, pyrrolidium, ammonium, phosphonium, and sulfonium and of anions with low Lewis basicities.[22] The ability to tailor the structure of ILs results in an extensive list of potential applications.

Ionic liquids have very distinctive properties, such as low melting point, wide liquid range, very low vapor pressure, nonvolatility, nonflammability, specific solvating strength and solubility, and good ionic conductivity.

Ionic liquids draw their liquid nature from a selection of ionic structures. Cations have weak intermolecular force, low symmetry, and a good distribution of charge while mostly, an increasing size of the anion with the same charge reduces the melting point.[23] These factors tend to reduce the lattice energy to form the crystalline of the salt.[24] Thus the very weak tendencies of ions to coordinate with oppositely charged ions make them liquid at low temperature, unlike typical salts. [24]

The ionic liquids are capable of being synthesized to meet a given application, which make them the designer solvents. It means that their properties can be tuned to suit the particular request for a process.[24] Understanding the basic rheological properties of the ionic liquids will undoubtedly be an aspect that will need to be considered when designing the ILs.

Chapter 4

AR G2 Rheometer from TA Instruments

All the rheological studies discussed within this document were conducted using an AR G2 rheometer from TA Instruments (New Castle, DE). Show below in Figure 4.1.

Figure 4-1. AR G2 rheometer equipped with an environmental testing chamber

The AR G2, at the moment, is considered to be a state-of-the-art rheometer. It utilizes an optical encoder to track the movement and exact position of the geometry. In addition, the bearing which provides the rotation is a magnetic bearing. Prior to starting the analysis, the instrument "maps" the selected geometry. During the mapping procedure the instrument tracks exactly how much torque is required to move the geometry over the entire 360 degrees of rotation. This type of information is used to adjust for any lack of absolute perfection that exists in the geometries construction, and calculate the amount of torque necessary for movement depending on the geometries exact location. The

instrument applies this torque correction to all measurements. Utilizing a magnetic bearing instead of an air bearing minimizes this correction and increases the instrument's sensitivity. The torque correction also takes into consideration the inertia of the geometry.

In addition to the mapping, the instrument determines the "zero gap" position. During this process the instrument is able to calibrate a normal force measurement. The normal force control allows the operator to set its value. This enables live time gap correction to correct for geometry expansion due to temperature and to adjust accordingly if the sample happens to extrude from the gap.

Chapter 5

Rheology of SFNs – Generation 1

The samples discussed within this chapter were synthesized by Dr. Zhmining Qiu. Dr. Qiu submitted six different batches of solvent-free nanofluids. These six samples were synthesized utilizing the approach described previously as generation 1. However, during the synthesis portion differing amounts of trimethoxy silane was utilized. The intention of utilizing the differing amounts of trimethoxy silane was to attempt to vary the thickness of the organic shell. The rheological analysis that follows was conducted to evaluate what effect the differing shell thicknesses would have on the SFN's rheology.

It is also worth mentioning that it was this study that gave rise to Professor John Texter's hypothesis that core free nanofluids (discussed in Chapter 7) may indeed be possible.

5.1 Oscillatory Rheology

5.1.1 NF105

The first SFNs material analyzed was synthesized to contain 105 ammonium surface modified groups per particle (lot 07-857-12). This material is hereafter referred to as NF105. To begin the analysis, a stress sweep was performed at 30^0C. The selected geometry was a 15mm 2^0 cone along with the Peltier plate. The acquisition parameters utilized a frequency of 1 Hz and varied stress from 100 μNm to 10,000 μNm. The instrument collected 10 datum points per decade; the point tolerance was set at 0.5% and time tolerance was set at 30 seconds. The ability to set a tolerance increases the reliability of the data. In this instance all data points collected are the average of three consecutive measurements where the values of the individual measurements fall within

0.5% of each other. If the condition of three consecutive measurements within 0.5% of each other is not met, then the instrument does not plot the data point and moves on to collect the next data point. The results from the stress sweep are shown in Figure 5-1.

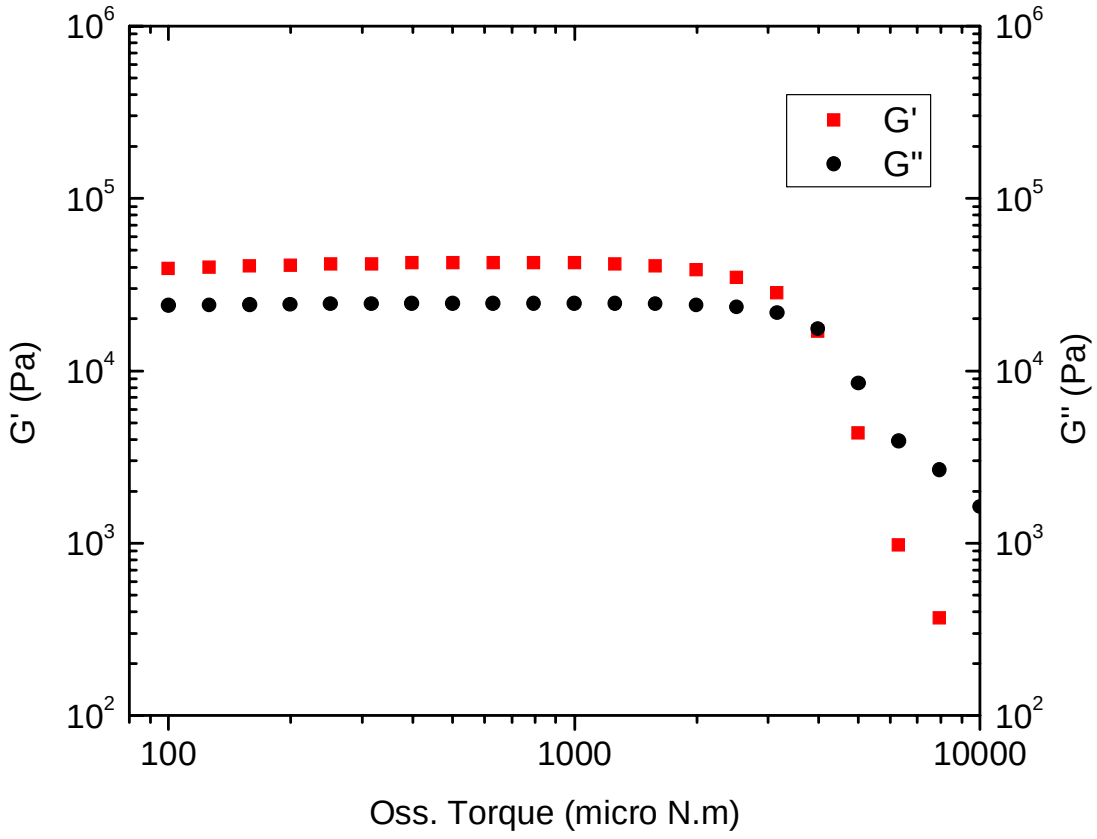

Figure 5-1. Stress sweep of NF105 at 30^0C

From the stress sweep, a portion of the linear viscoelastic range (LVR) is revealed. When using a frequency of 1 Hz and the temperature of 30^0C, the data indicate that using an oscillation torque of 100 to 1100 μNm will be within the LVR. The LVR is the region where the storage and loss modulus are both constant and parallel with each while the torque is varied.

Another stress sweep was conducted at 80^0C using the same acquisition parameters described above, except the temperature and the range of applied stress was from 50 to 1,200 μNm. The results of the stress sweep are shown in Figure 5-2.

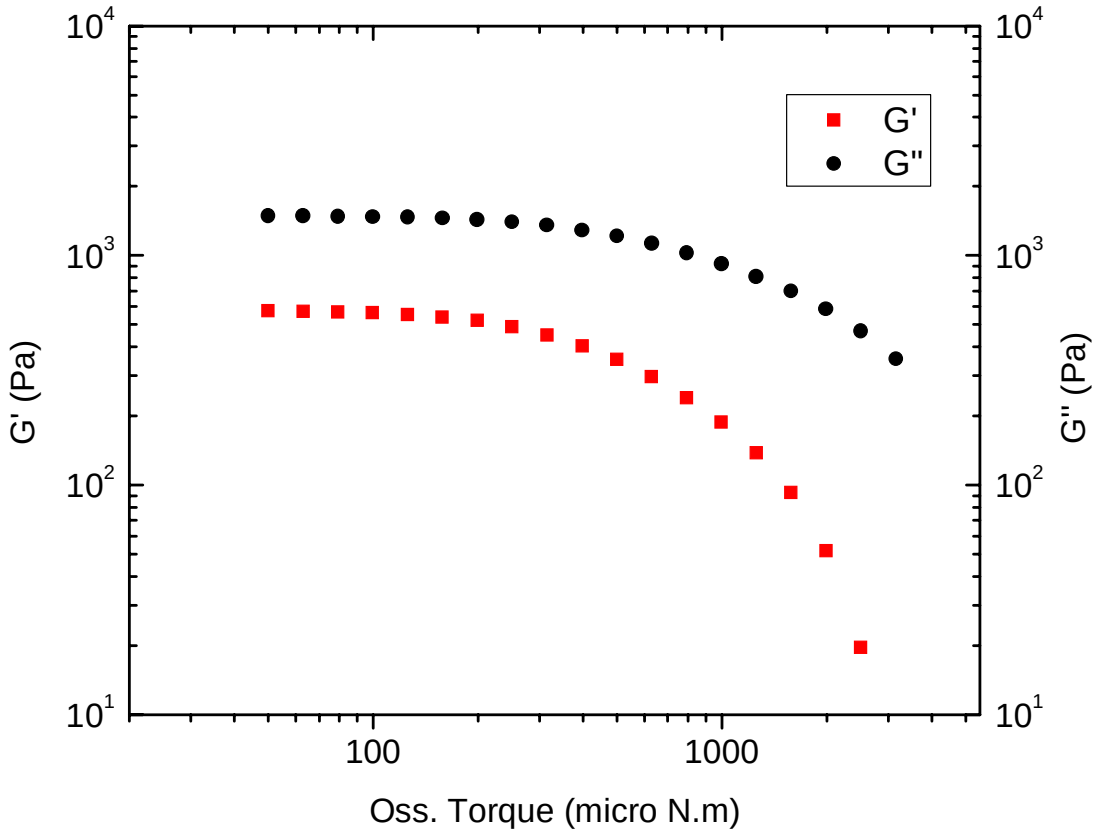

Figure 5-2. Stress sweep of NF105 at 80^0C

Next the stability of NF105 was examined using a time sweep. The selected geometry was a 15mm 2^0 cone along with the Peltier plate. The acquisition parameters for the time sweep used a temperature of 80^0C, an oscillation torque of 100 μNm, and a frequency of 1 Hz. The experiment was conducted over a ten-minute period, and a datum point was collected every ten seconds. The time sweep is presented in Figure 5-3.

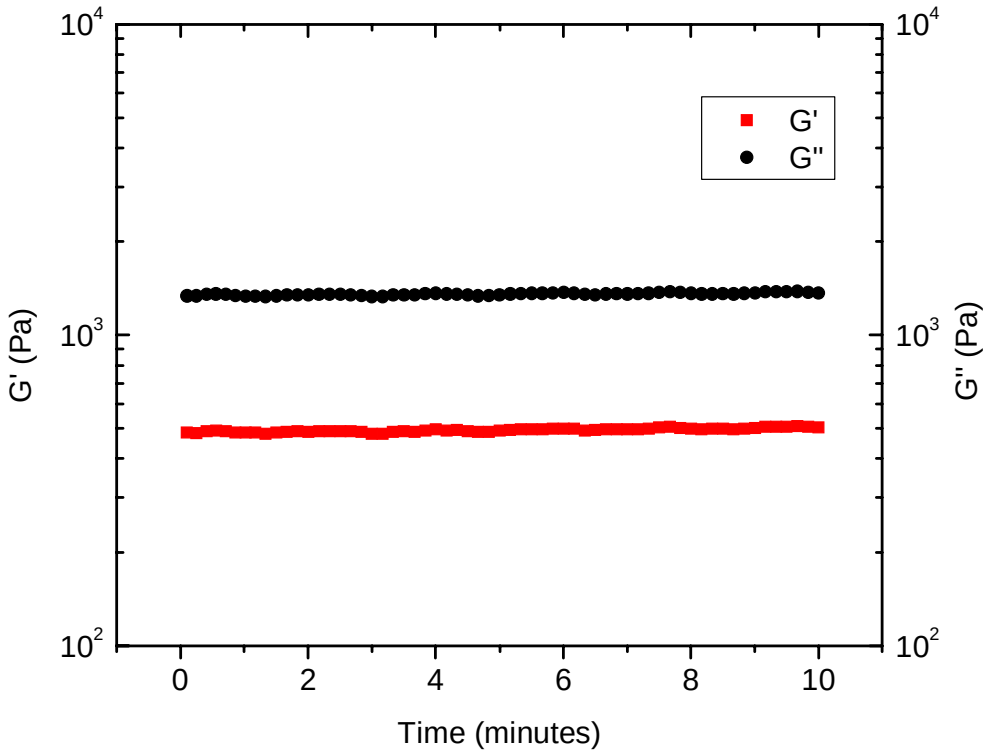

Figure 5-3. Time sweep of NF105 at 70^0C

The data presented in the time sweep revealed that the sample is stable over the acquisition parameters. The conclusion is based on the fact that the storage and loss modulus are essentially constant and parallel with each other.

The three previously described experiments were conducted to gain information on the acquisition parameters required to conduct a temperature sweep. One of, if not the, most attractive feature of SFNs is the fact that they exhibit liquid-like behavior without the absence of solvent. NF105 is extremely high in viscosity at room temperature. A temperature sweep will indicate at what temperature the material begins to readily exhibit liquid-like properties.

The chosen acquisition parameters for the temperature sweep are a frequency of 1 Hz and an oscillation torque of 100 μNm. Please note that the chosen oscillation torque of 100 μNm was selected because it was within the LVR at both 30 and 80^0C. The temperature range chosen was 20 to 80^0C with datum points taken every 1^0C. A 2-minute equilibration period was given at every temperature interval. The selected geometry was a 15mm 2^0 cone along with the Peltier plate. The results are shown in Figure 5-4.

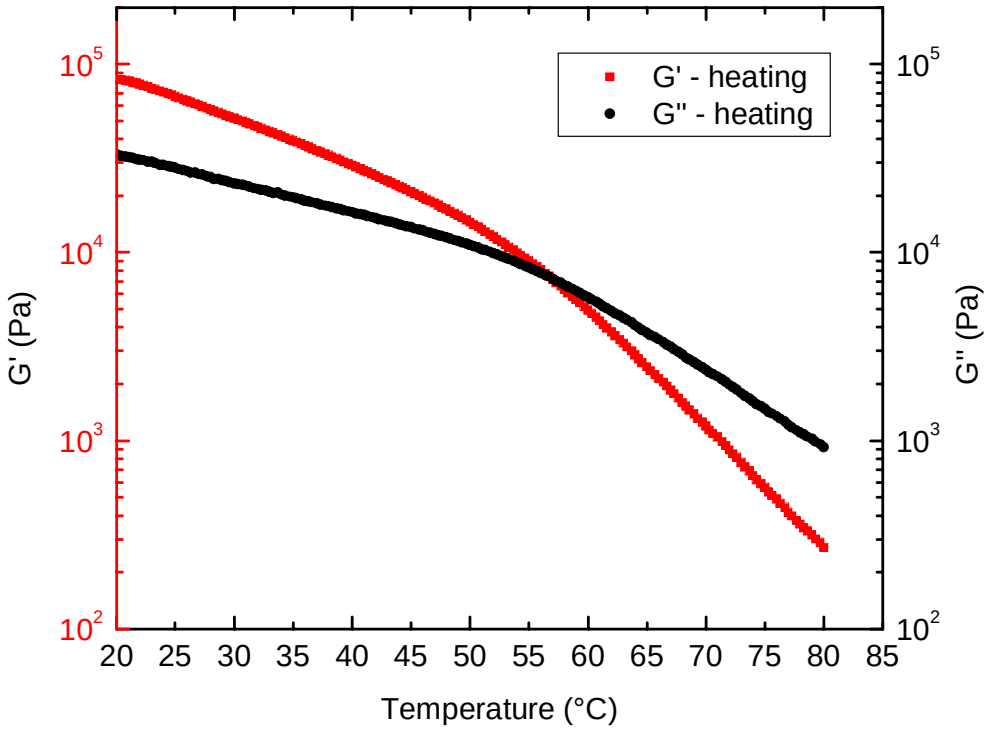

Figure 5-4. Temperature sweep of NF105

The data indicate that the material is very temperature dependent, with changes in the storage moduli of 2 orders of magnitude over a 60^0C temperature range. The data also

indicate that the material readily exhibits liquid-like properties at 57^0C, as that is the temperature where the loss modulus becomes greater than the storage modulus.

5.1.2 NF205

The second SFNs material analyzed was synthesized in a manner intended to generate 205 ammonium surface modified groups per particle (lot 08-961-14). Hereafter SFNs lot 08-961-14 will be referred to as NF205. To begin the analysis, a stress sweep was performed at 30^0C. The selected geometry was a 15mm 2^0 cone along with the Peltier plate. The acquisition parameter utilized was a frequency of 1 Hz. The stress was varied from 10 μNm to 1,300 μNm. The instrument collected 10 datum points per decade. The point tolerance was set at 0.5% and time tolerance was set at 30 seconds. The results from the stress sweep are shown in Figure 5-5.

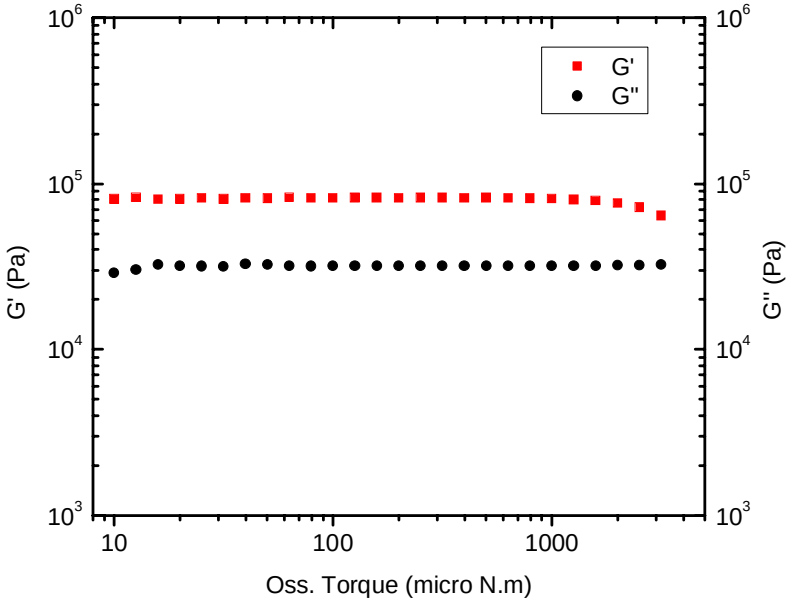

Figure 5-5. Stress sweep of NF205 at 30^0C

From the stress sweep, a portion of the linear viscoelastic range (LVR) is revealed. When using a frequency of 1 Hz and the temperature of 30^0C, the data indicate that using an oscillation torque of 20 to 1000 μNm will be within the LVR.

The chosen acquisition parameters for the temperature sweep are a frequency of 1 Hz and an oscillation torque of 100 μNm. Please note that the chosen oscillation torque of 100 μNm was selected because it was within the LVR at 30^0C. The temperature range chosen was 25 to 80^0C with data points taken every 2^0C. A 2-minute equilibration period was given at every temperature interval. The selected geometry was a 15mm 2^0 cone along with the Peltier plate. The results are shown in Figure 5-6.

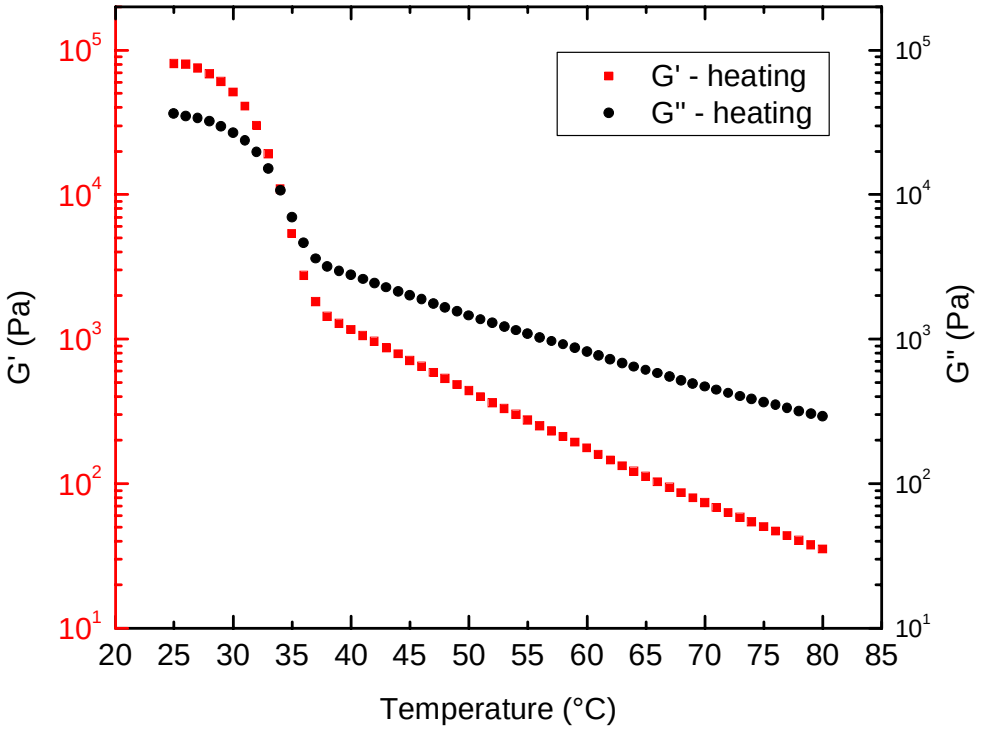

Figure 5-6. Temperature sweep for NF205

The data indicate that the material's response to temperature is extreme between 25 to 40^0C. The data also indicate that the material readily exhibits liquid-like properties at 34^0C, as that is the temperature where the loss modulus becomes greater than the storage modulus.

5.1.3 NF275

The third SFNs material analyzed was synthesized to contain 275 ammonium surface modified groups per particle (lot 08-961-49). Hereafter, SFNs lot 08-961-49 will be referred to as NF275. To begin the analysis, a stress sweep was performed at 25^0C. The selected geometry was a 15mm 2^0 cone along with the Peltier plate. The acquisition parameters utilized was a frequency of 1 Hz. The stress was varied from 1 μNm to 300 μNm. The instrument collected 10 data points per decade. The point tolerance was set at 0.5% and time tolerance was set at 30 seconds. The results from the stress sweep are shown in Figure 5-7.

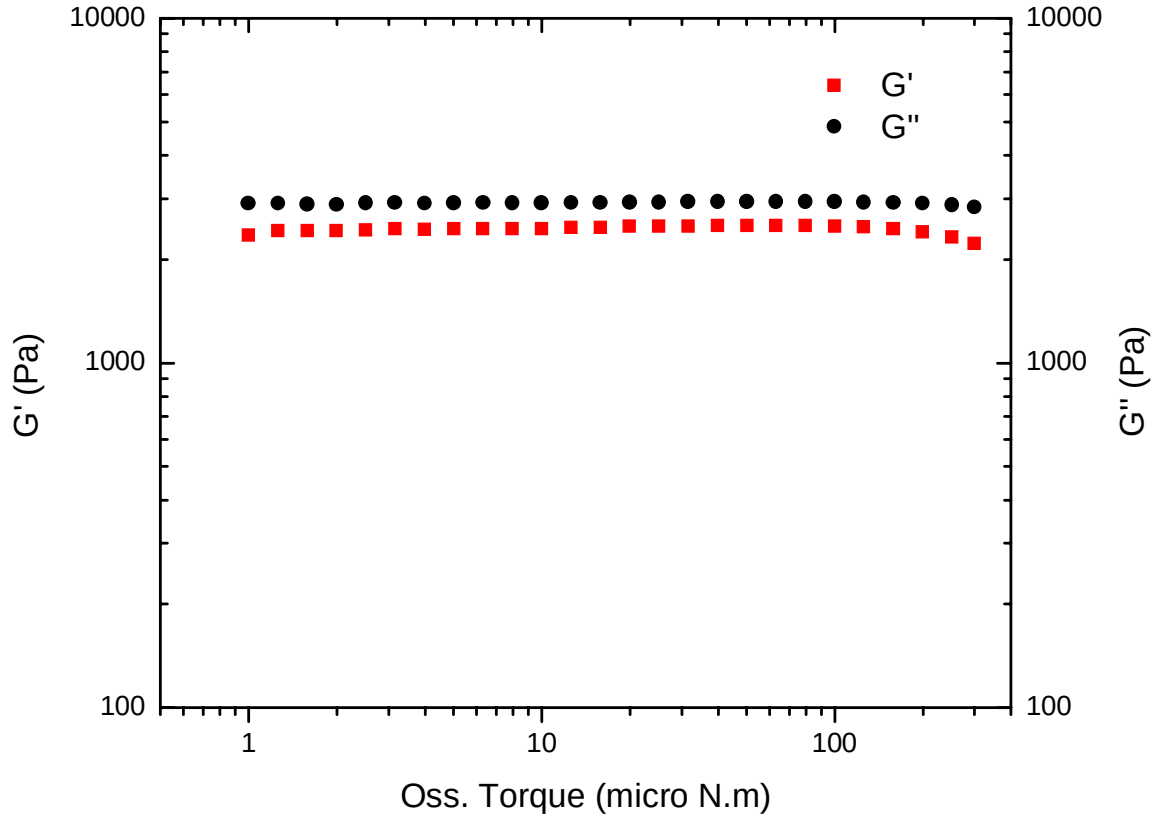

Figure 5-7. Stress sweep of NF275 at 25^0C

Another stress sweep was conducted at 70^0C using the same acquisition parameters described above, except the temperature and the range of applied stress was from 1 to 1000 μN m. The results of the stress sweep are shown in Figure 5-8.

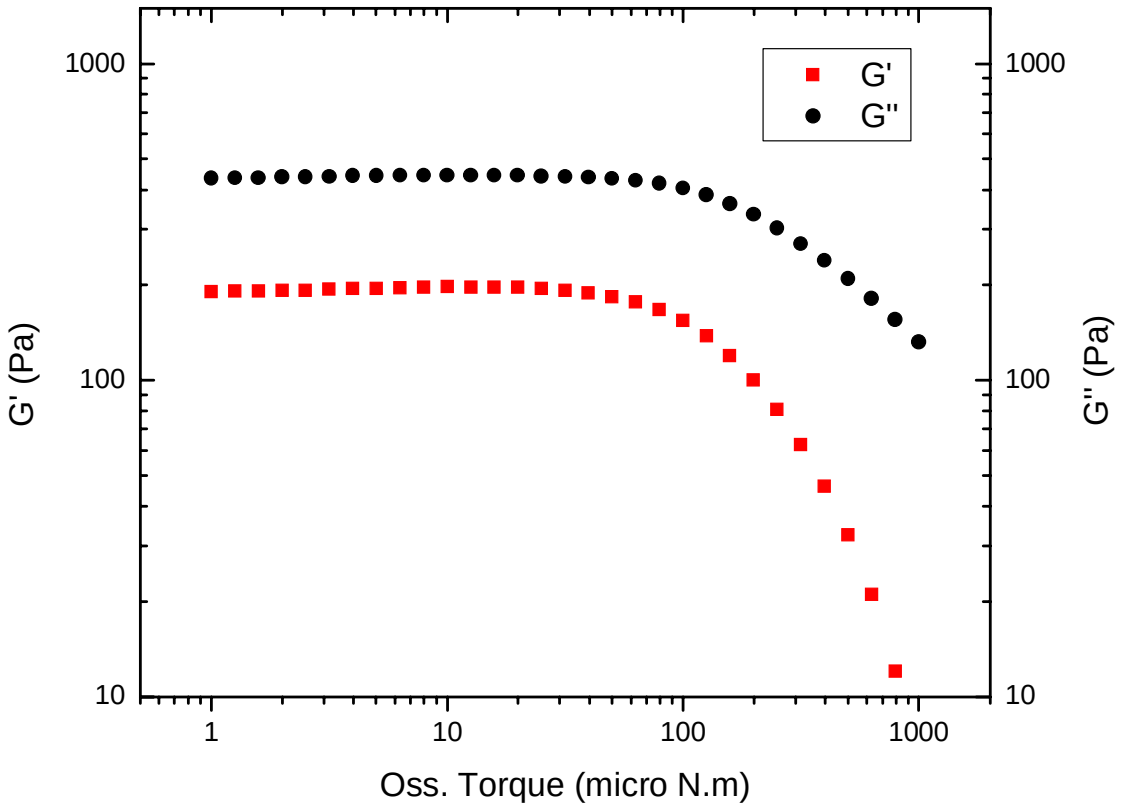

Figure 5-8. Stress sweep of NF275 at 70^0C

The data from the both stress sweeps indicate that at a temperature range of 25 to 70^0C, the overlapping LVR is 1 to 40 μNm.

Next the stability of NF275 was examined using a time sweep. The selected geometry was a 15mm 2^0 cone along with the Peltier plate. The acquisition parameters for the time sweep used a temperature of 70^0C, an oscillation torque of 10 μNm, and a frequency of 1 Hz. The experiment was conducted over a ten-minute period, and a data point was collected every ten seconds. The time sweep is presented in Figure 5-9.

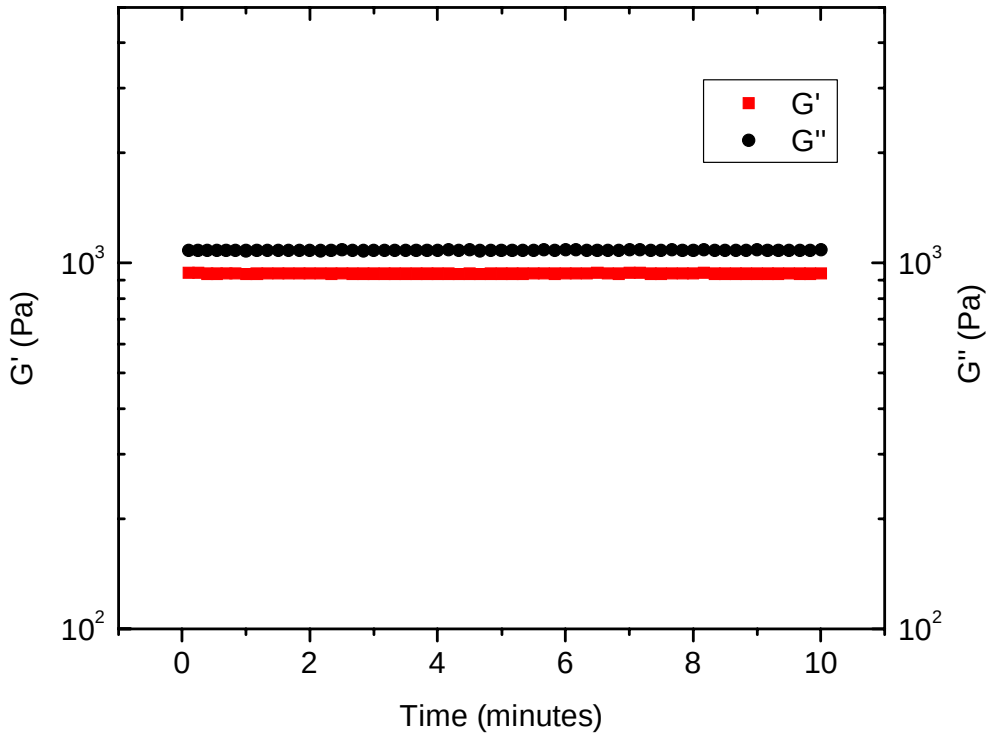

Figure 5-9. Time sweep of NF275 at 70^0C

The data indicate that the stability of the sample is not an issue. The chosen acquisition parameters for the temperature sweep are a frequency of 1 Hz and an oscillation torque of 10 μNm. The temperature range chosen was 25 to 75^0C with data points taken every 1^0C. A 2-minute equilibration period was given at every temperature interval. The selected geometry was a 15mm 2^0 cone along with the Peltier plate. The results are shown in Figure 5-10.

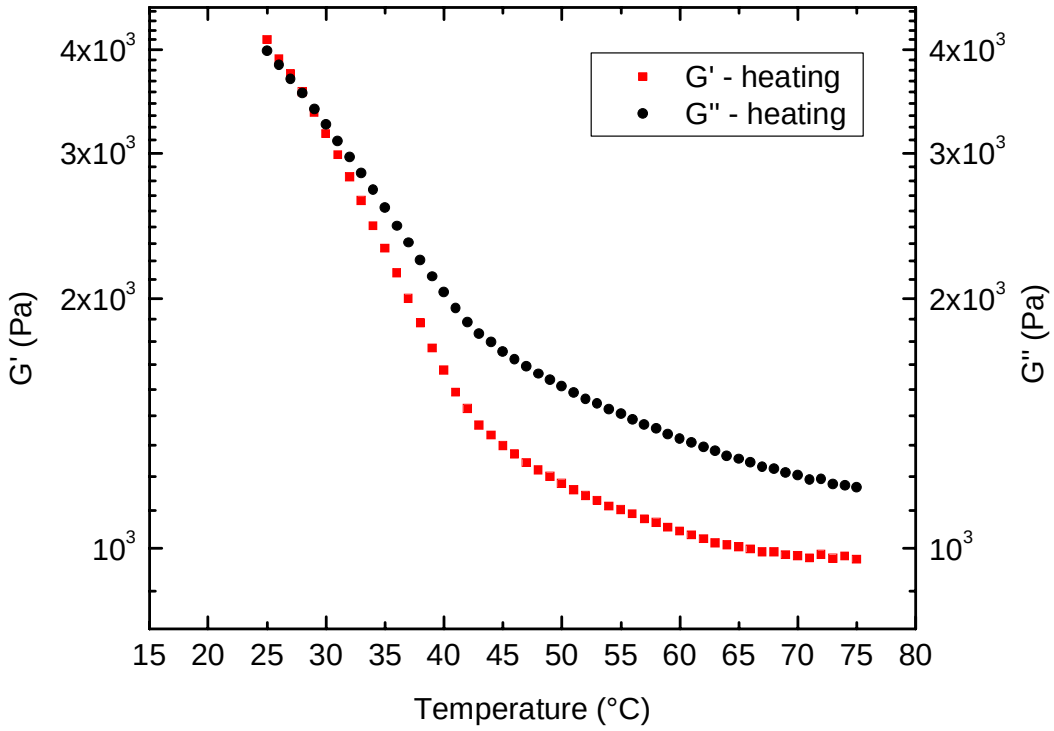

Figure 5-10. Temperature sweep of NF275

The data indicate that the material's response to temperature is relatively mild over 25 to 75^0C (especially compared to the previously analyzed SFNs). The data also indicate that the material readily exhibits liquid-like properties at 28^0C, as that is the temperature where the loss modulus becomes greater than the storage modulus.

5.1.4 NF395

The third SFNs material analyzed was synthesized to contain 395 ammonium surface modified groups per particle (lot 08-988-22). Hereafter, SFNs lot 08-988-22 will be referred to as NF395.

To begin the analysis, a stress sweep was performed at 20^0C. The selected geometry was a 15mm 2^0 cone along with the Peltier plate. The acquisition parameter utilized was a frequency of 1 Hz. The stress was varied from 1 μNm to 300 μNm. The instrument collected 10 datum points per decade. The point tolerance was set at 0.5% and time tolerance was set at 30 seconds. The results from the stress sweep are shown in Figure 5-11.

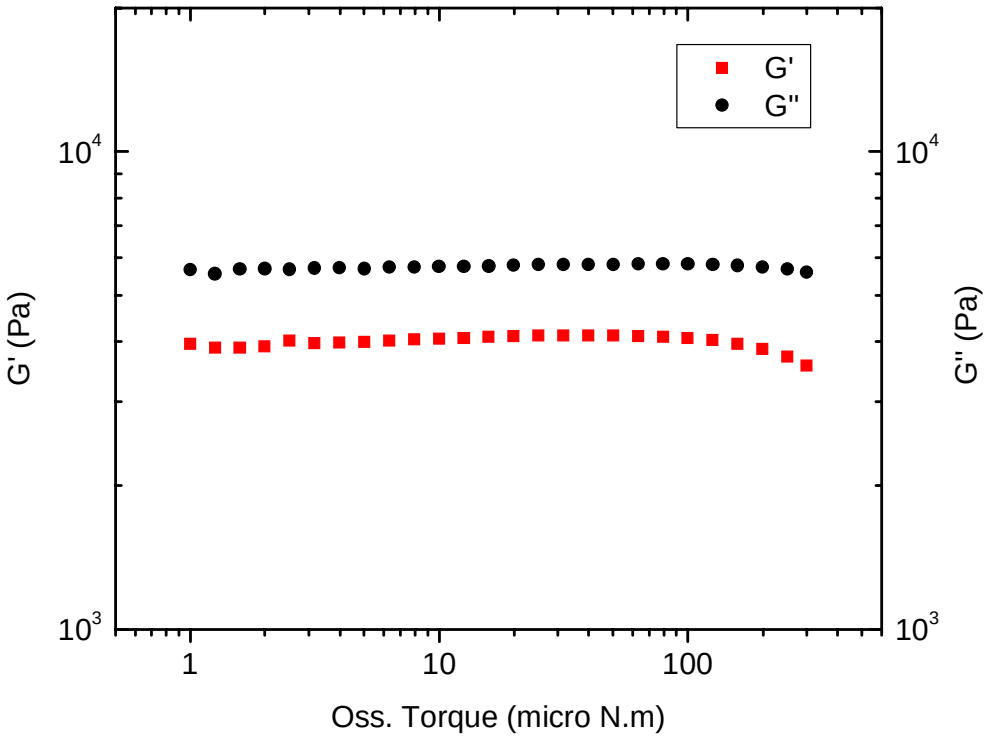

Figure 5-11. Stress sweep for NF395 at 5^0C

Another stress sweep was conducted at 70^0C using the same acquisition parameters described above, except the temperature, and the range of applied stress was from 1 to 400 μNm. The results of the stress sweep are shown in Figure 5-12.

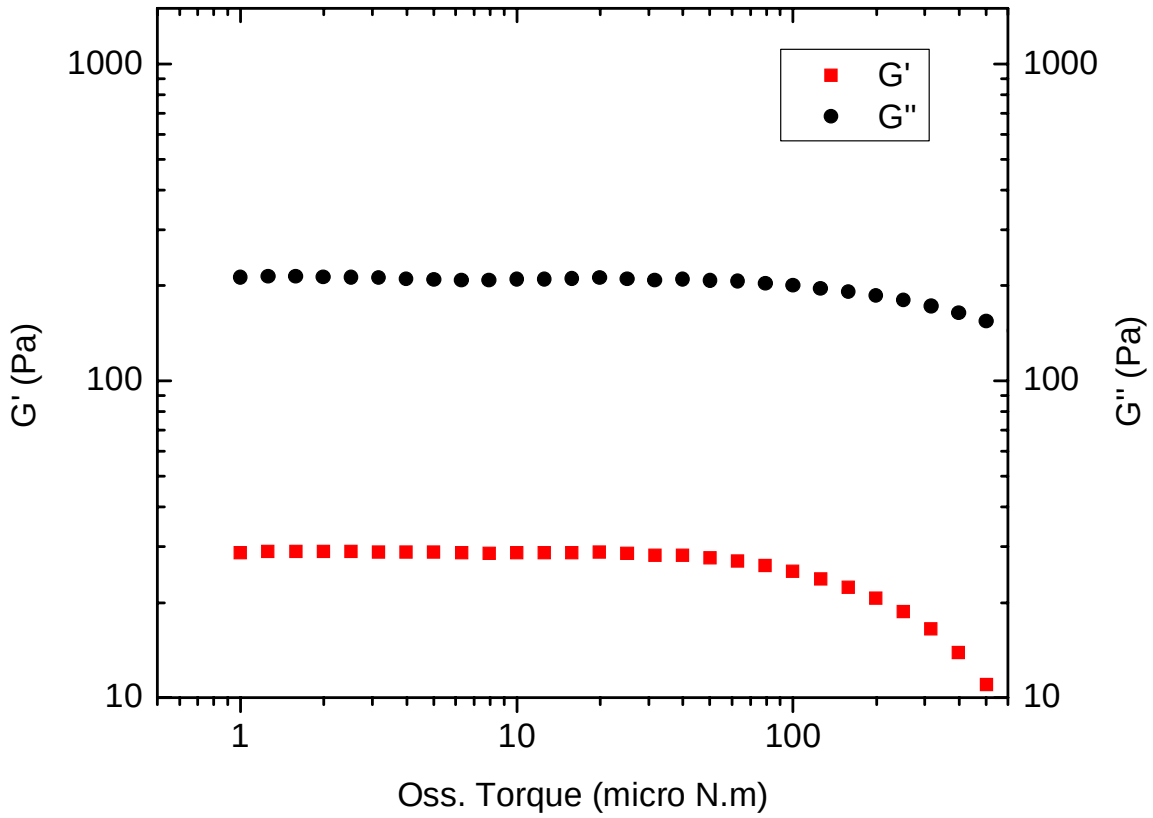

Figure 5-12. Stress sweep for NF395 at 70^0C

The data from the both stress sweeps indicate that at a temperature range of 5 to 70^0C, the overlapping LVR is 1 to 60 μNm.

Next the stability of NF395 was examined using a time sweep. The selected geometry was a 15mm 2^0 cone along with the Peltier plate. The acquisition parameters for the time sweep used a temperature of 60^0C, an oscillation torque of 10 μNm, and a frequency of 1 Hz. The experiment was conducted over a ten-minute period, and a datum point was collected every ten seconds. The time sweep is presented in Figure 5-13.

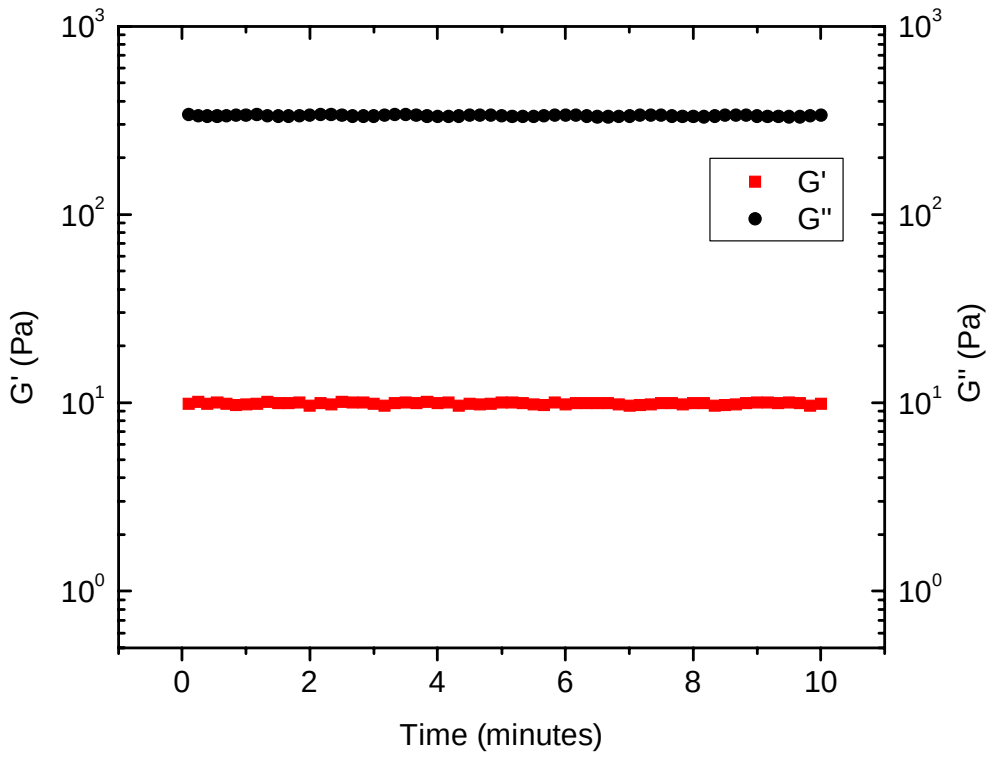

Figure 5-13. NF375 at 60^0C

The data obtained in the time sweep indicate that the sample is indeed stable. The chosen acquisition parameters for the temperature sweep are a frequency of 1 Hz and an oscillation torque of 10 μNm. The temperature range chosen was 5 to 60^0C with data points taken every 1^0C for the interval 0-20^0C and 5^0C increments for the remainder of the analysis. A 2-minute equilibration period was given at every temperature interval. The selected geometry was a 15mm 2^0 cone along with the Peltier plate. In addition, the nitrogen purge apparatus was installed for this analysis. The nitrogen purge simply evacuates the air in the area surrounding the sample. Performing this analysis without the nitrogen purge results in moisture condensing on the Peltier plate at the lower temperature range. The results are shown in Figure 5-14.

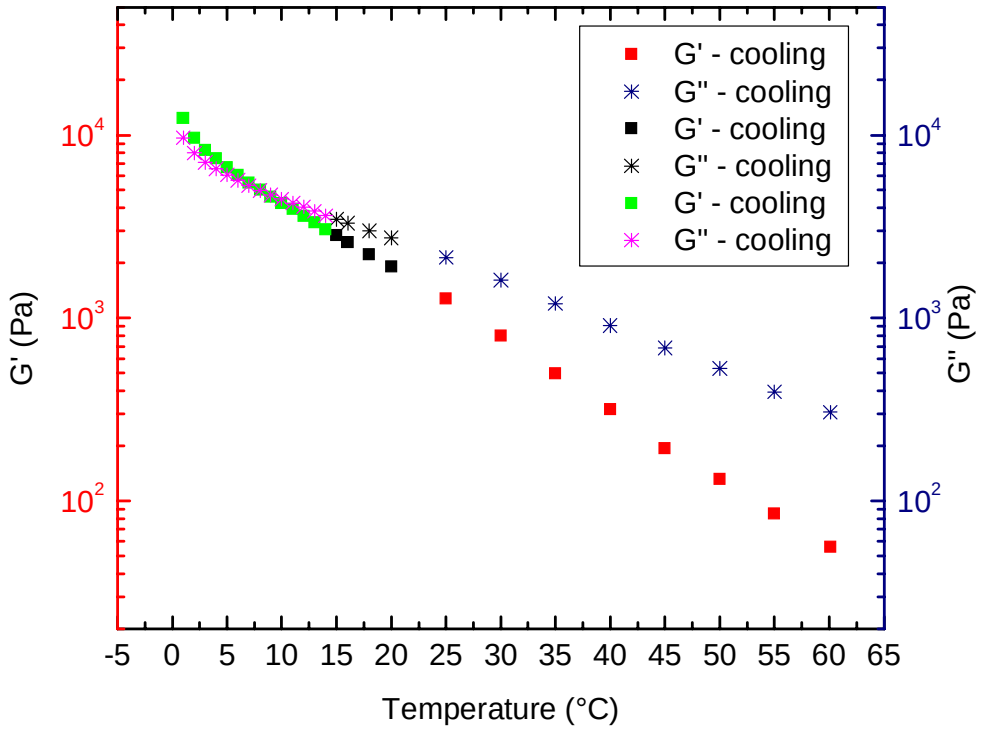

Figure 5-14. Temperature sweep for NF395

The data from the temperature sweep indicate that the material exhibits liquid like properties at 6^0C. It should also be noted that the presented data are the result of multiple runs. The initial acquisition parameters were not adequate to capture the point where the storage and loss modulus intersected. Once that was detected, the temperature sweep was lowered in temperature, but the higher data points were not repeated.

5.1.5 NF1110

This SFNs material analyzed was synthesized to contain 1110 ammonium surface modified groups per particle (lot 08-988-25). Hereafter, SFNs lot 08-988-25 will be referred to as NF1110.

To begin the analysis, a stress sweep was performed at 20^0C. The selected geometry was a 25mm parallel plate along with the environmental testing chamber. The environmental testing chamber is an accessory that is placed on the ARG2. It places the sample in an insulated chamber that contains a furnace for heating and liquid nitrogen fitting for cooling to low temperatures. The acquisition parameters utilized were a frequency of 1 Hz. The stress was varied from 1 μNm to 1000 μNm. The instrument collected 10 datum points per decade. The point tolerance was set at 0.5%, and time tolerance was set at 30 seconds. The results from the stress sweep are shown in Figure 5-15.

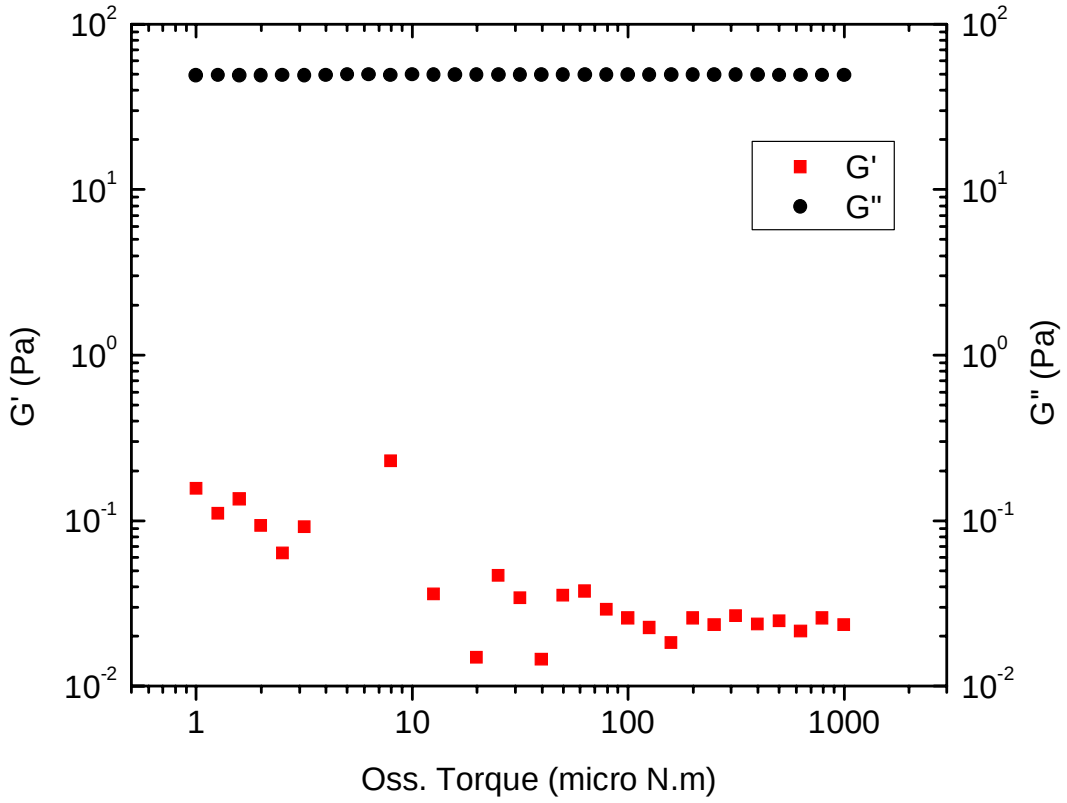

Figure 5-15. Stress sweep of NF1110 at 20^0C

The results from the stress sweep were like none we have observed thus far. The data indicate that the storage modulus is essentially 0 Pa at 20^0C. Additionally, the delta degrees from the analysis were 90. Delta degrees is a value that the instrument records that gives an indication whether the material is responding in a more viscous or elastic manner. A delta degree value of 90 indicates a purely viscous response, and hence that explains the erratic readings of the storage modulus.

The chosen acquisition parameters for the temperature ramp are a frequency of 1 Hz and an initial oscillation torque of 10 μNm. An additional condition was added to the torque control. If the torque fell outside of the 0.5% tolerance, the instrument would revert to a 0.1% strain control. Controlling the sample by strain is advantageous when drastic differences in viscosity are expected or when analyzing near solid material. The temperature range chosen was 100 to -100^0C with data points taken every 0.5^0C and a temperature ramp of 3^0C/minute. The selected geometry was a 25mm parallel plate along with the environmental testing chamber. The results are shown in Figure 5-16.

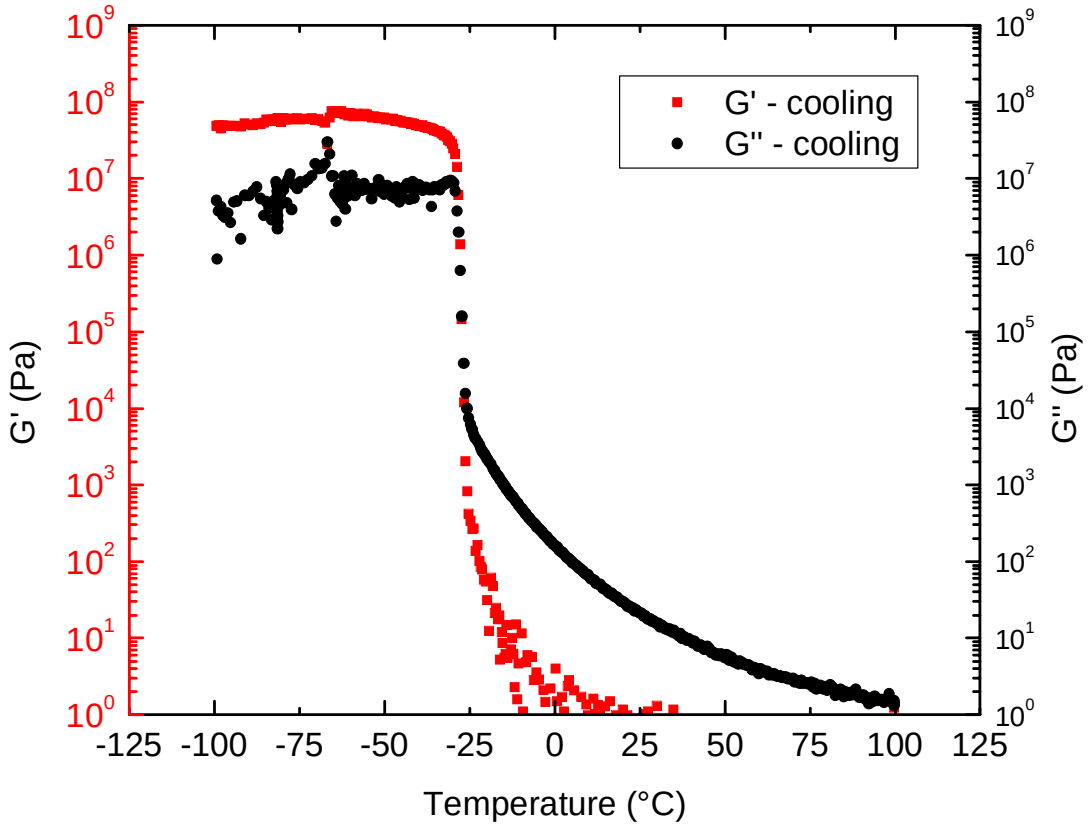

Figure 5-16. Temperature sweep for NF1110

The results from the data indicated that the material exhibits liquid-like behavior starting at -25^{0}C. In addition the Tg was detected at -64^{0}C. The Tg can be clearly observed as the storage modulus decreases at that very point, and the loss modulus spikes at the same temperature.

5.1.6 Oscillatory Rheology Discussion

The solvent-free nanofluids examined exhibited a wide range of rheological properties. The selected acquisition parameters chosen were capable of detecting the linear viscoelastic range in all of the samples except NF1110. The stress sweep of

NF1110 at room temperature resulted in a completely viscous response, as shown by the high degree of fluctuation of the storage modulus. The time sweeps conducted on all of the samples indicated that each sample appeared to be stable over the chosen acquisition parameters. The intention in conducting the oscillatory testing was to determine at what temperature the samples begin to exhibit liquid-like properties and to generate some data that may lead help fine tune future formulations. It was quite apparent that increasing the amount of ammonium groups on the surface of the nanoparticles resulted in materials that exhibited liquid-like properties at lower temperatures.

5.2 Rotational Measurements

The solvent-free nanofluids discussed in Chapter 5 and one additional batch containing 370 ammonium surface modified groups per particle were analyzed using rotational rheology. The rationale behind conducting rotational rheology was to attempt to collect zero shear viscosity data. As discussed in Chapter 1, zero shear viscosity measurements are possible when the sample being analyzed can with stand a small amount of stress prior to yielding. The viscosity recorded from the zero shear plateau, also referred to as the first Newtonian plateau, is representative of the viscosity of the sample at rest. It is convenient to discuss and compare this type of viscosity, because it eliminates the need to specify the shear rate it was taken with or the geometry used for the data collection. As discussed below, careful data interpretation and review are necessary when discussing zero shear viscosity, because one method will likely not be sufficient to access the viscosity of samples of different viscosities.

5.2.1 NF105

The following rotational method was developed to report the viscosity from the first Newtonian plateau of NF105. The selected geometry was a 15mm 2^0 cone along with the Peltier plate. The method consisted of shearing the sample from 0.0005 s^{-1} to 2 s^{-1}. Ten datum points were taken per decade during the shear ramp. The measurements were conducted from 30 to 80^0C at 5^0C increments. A 10-minute equilibration period was given at each interval. The results of the analysis are presented in Figure 5-17.

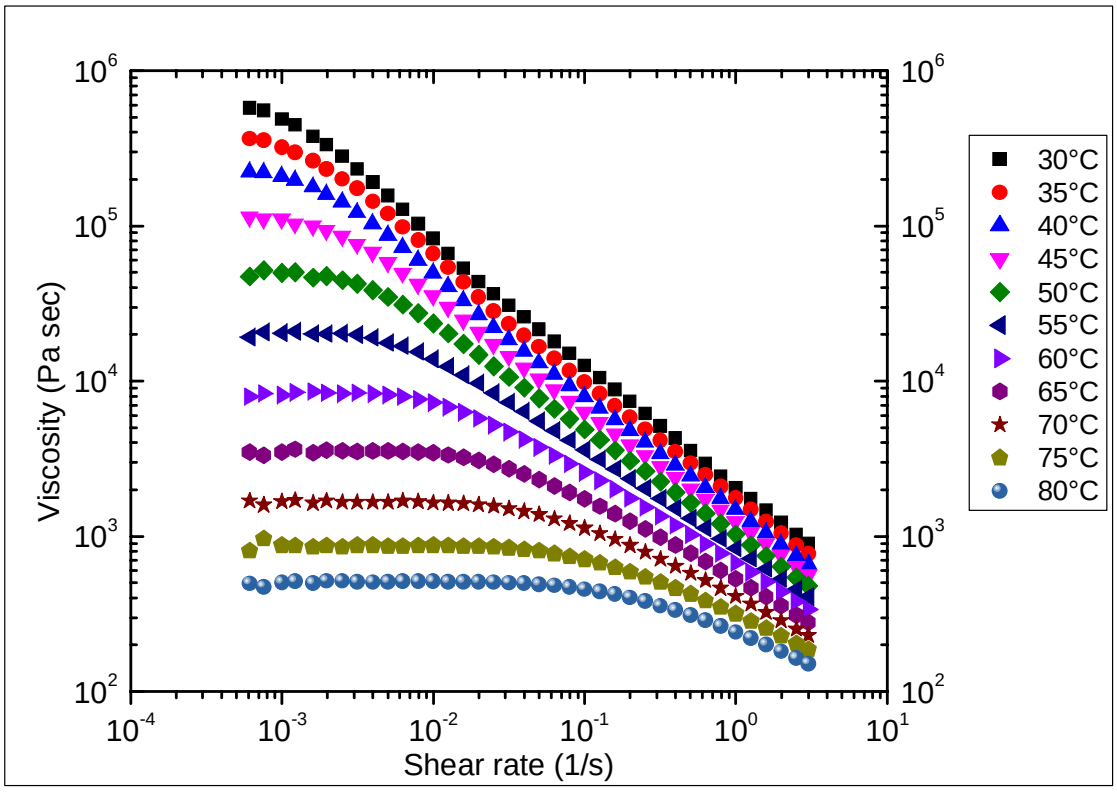

Figure 5-17. Flow curves for NF105

The above data do indicate that is possible to report zero shear viscosity values for NF105. The plateau can be viewed by looking at the viscosity data points that are

relatively constant at the low shear rate values. The viscosity values reported in Table 5-1 were taken from that region.

Table 5-1: Zero shear viscosity values for NF105

NF105	
Temperature (^{0}C)	Viscosity (Pa S)
30	555200
35	363500
40	223200
45	113200
50	51570
55	20480
60	8414
65	3642
70	1692
75	855
80	513

5.2.2 NF205

The following rotational method was developed to report the viscosity from the first Newtonian plateau of NF205. The selected geometry was a 15mm 2^0 cone along with the Peltier plate. The method consisted of shearing the sample from 0.001 s^{-1} to 0.5 s^{-1}. Ten datum points were taken per decade during the shear ramp. The measurements were conducted from 30 to 80^{0}C at 10^{0}C increments. A 10-minute equilibration period was given at each interval. The results of the analysis are presented in Figure 5-18.

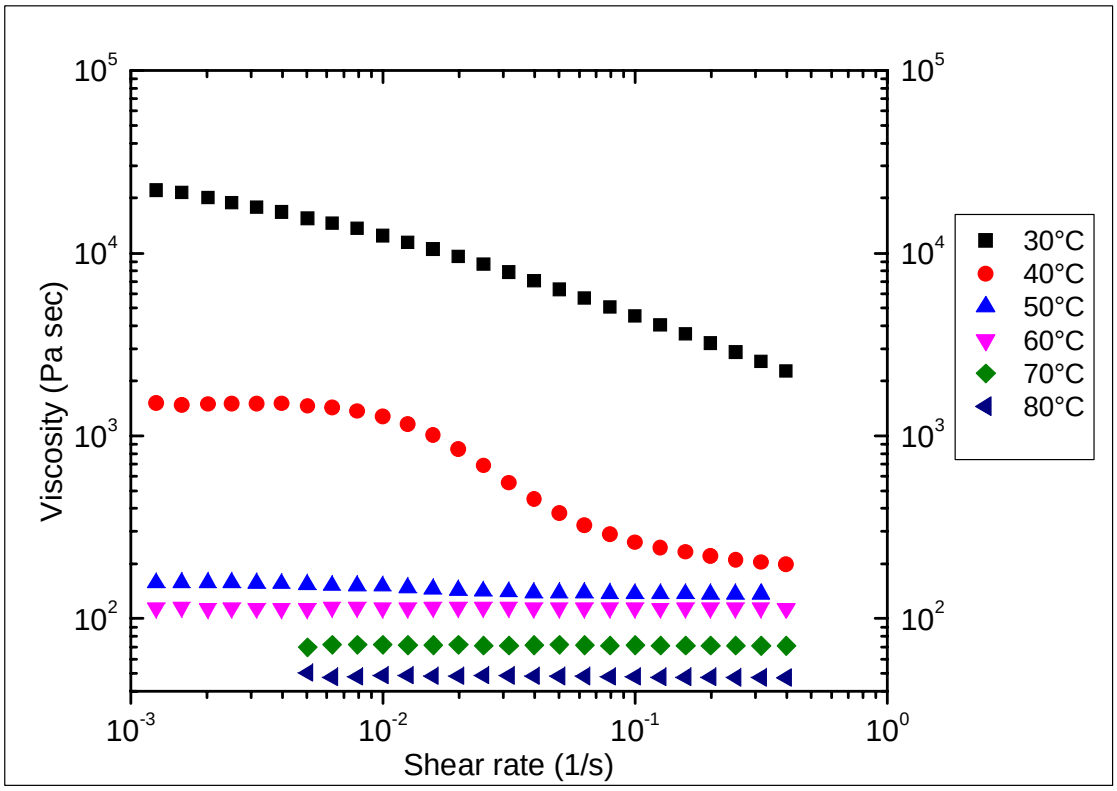

Figure 5-18. Flow curves for NF205

The zero shear viscosity values are listed in Table 5-2. The extreme temperature dependence shown in the oscillation temperature sweep between 30 and 50^0C is again observed during the rotational viscosity analysis.

Table 5-2. Zero shear viscosity values for NF205

NF205	
Temperature (^{0}C)	Viscosity (Pa S)
30	38800
40	1533
50	156
60	115
70	72
80	49

5.2.3 NF275

The following rotational method was developed to report the viscosity from the first Newtonian plateau of NF275. The selected geometry was a 15mm 2^0 cone along with the Peltier plate. The method consisted of shearing the sample from 0.001 s^{-1} to 3 s^{-1} for the temperatures of 25-40^{0}C. The shear rate for the temperatures of 45-80^{0}C was from 0.01 s^{-1} to 3 s^{-1}. The measurements were conducted from 25 to 75^{0}C at 5^{0}C increments. A 10-minute equilibration period was given at each interval. Ten data points were taken per decade during the shear ramp. The results of the analysis are presented in Figure 5-19.

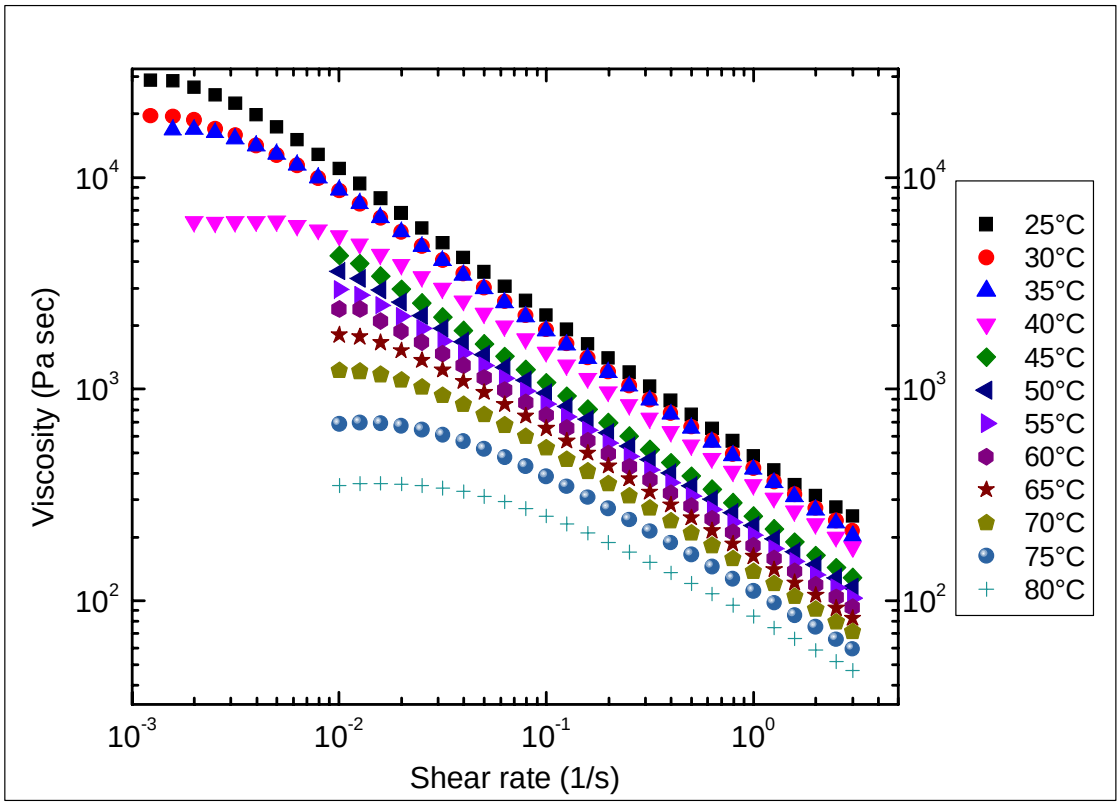

Figure 5-19. Flow curves for NF275

The zero shear viscosity values are listed in Table 5-3.

Table 5-3. Zero shear viscosity values for NF275

NF275	
Temperature (^{0}C)	Viscosity (Pa S)
25	28780
30	19550
35	18720
40	6280
45	5622
50	4277
55	2955
60	2392
65	1797
70	1221
75	683
80	359

5.2.4 NF370

The following rotational method was developed to report the viscosity from the first Newtonian plateau of NF370. It is worth mentioning that viscosity determination was the only requested analysis for NF370 (lot 08-961-97), and thus this batch is not discussed in Chapter 5. The selected geometry was a 15mm 2^0 cone along with the Peltier plate. The method consisted of shearing the sample from 0.01 s^{-1} to 10 s^{-1} for the temperatures of 25-40^{0}C. The shear rate for the temperatures of 45-80^{0}C was from 0.01

s^{-1} to 3 s^{-1}. The measurements were conducted from 25 to 70^{0}C at 5^{0}C increments. A 10-minute equilibration period was given at each interval. Ten data points were taken per decade during the shear ramp. The results of the analysis are presented in Figure 5-20, and resulting zero shear viscosity values are presented in Table 5-4.

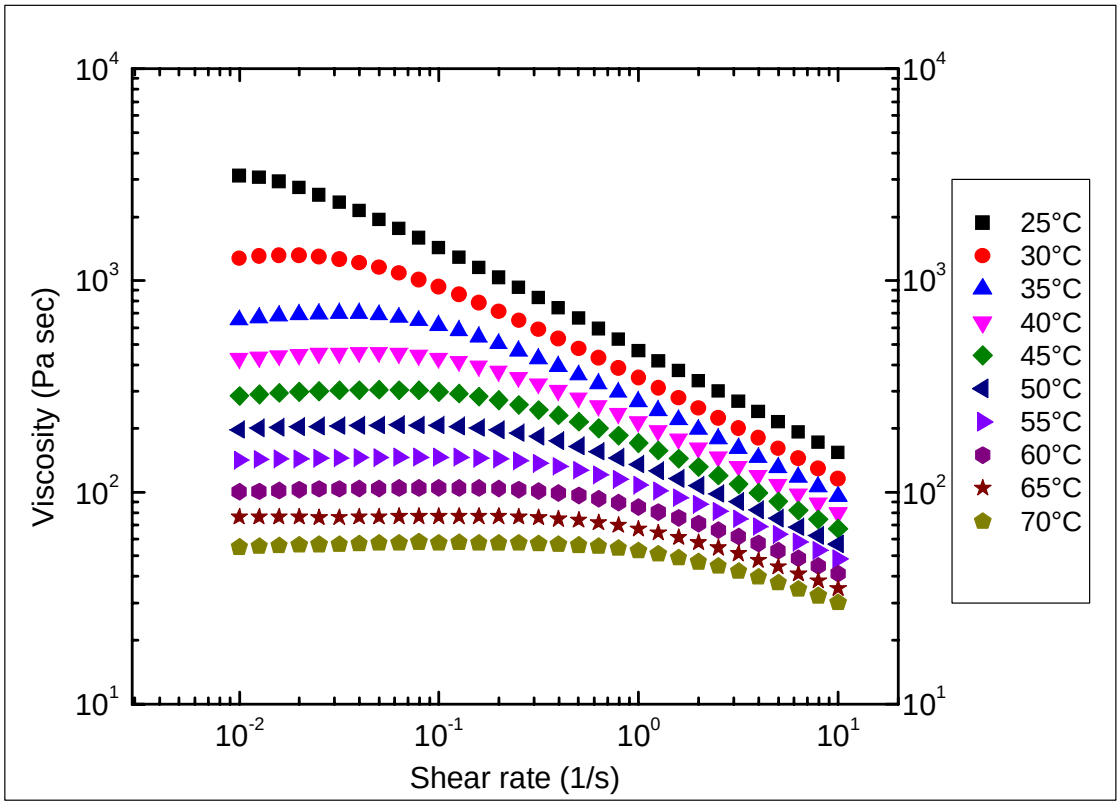

Fi

Figure 5-20. Flow curves for NF370

The resulting zero shear viscosity values are provided in Table 5-4.

Table 5-4. Zero shear viscosity values for NF370

NF370	
Temperature (^{0}C)	Viscosity (Pa S)
25	3117
30	1314
35	698
40	451
45	302
50	207
55	145
60	104
65	77
70	57

5.2.5 NF395

The following rotational method was developed to report the viscosity from the first Newtonian plateau for NF395. The selected geometry was a 15mm 2^0 cone along with the Peltier plate. The method consisted of shearing the sample from 0.1 s^{-1} to 3 s^{-1} for the temperatures of 20-70^{0}C. The measurements were conducted in 5^{0}C increments. A 10-minute equilibration period was given at each interval. Ten data points were taken per decade during the shear ramp. The results of the analysis are presented in Figure 5-21.

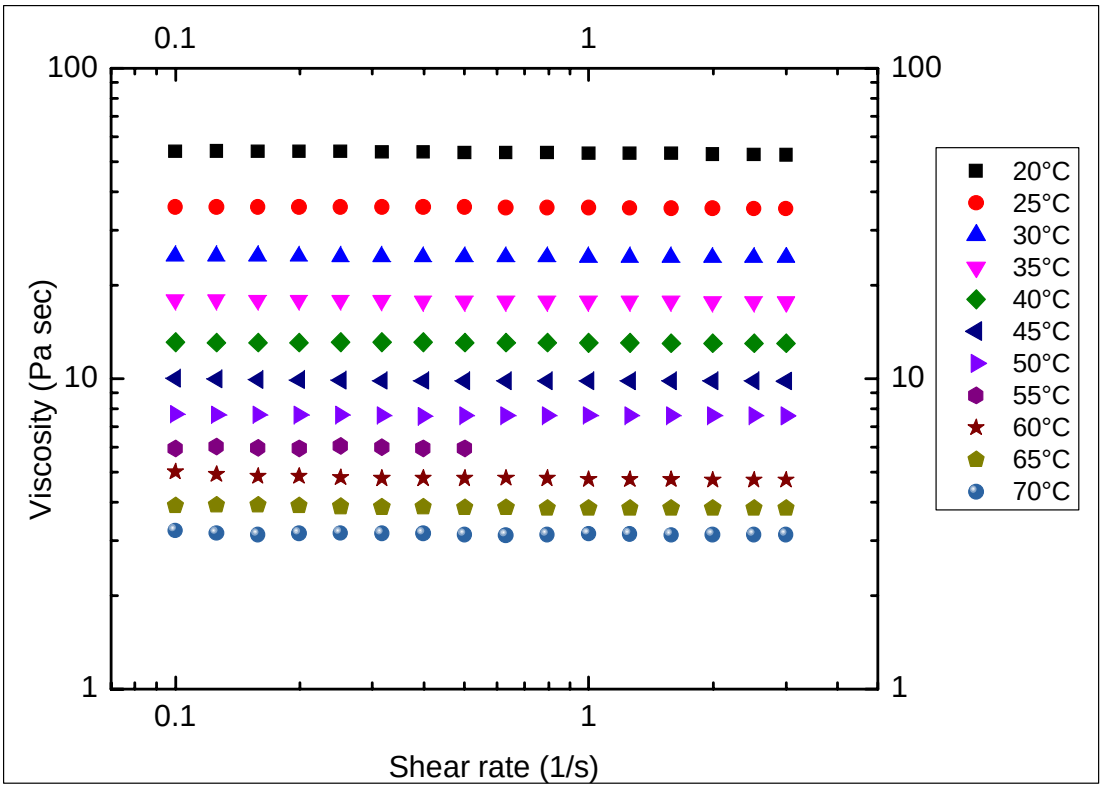

Figure 5-21. Flow curves for NF395

This particular lot appeared to display Newtonian flow properties over the given shear range. Utilizing a shear rate below 0.1 s^{-1} resulted in the instrument rejecting the data points. A rejection occurs when the replicate threshold is not met. The replicate threshold is a value that is manually set that rejects data point when three consecutive measurements are outside of the value. The replicate threshold was set at 5% for all of the samples discussed in this analysis. Looking at the rotational data alone does not provide any explanation as to why values below 0.1 s^{-1} were not possible. However, comparing the oscillatory data may provide some insight. NF395 has the lowest storage moduli of the sample discussed in this chapter thus far. The inability for the sample to hold its structure under low shear is directly related to its storage modulus. This

occurrence is a nice illustration why coupling oscillatory and rotational testing can be insightful. Last, it is worth noting that increasing the shear rate past 3^{-s} resulted from the sample coming. Ideally, the sample would have been placed in the cuvette sample chamber. However, in order for the cuvette to be utilized, a sample volume of 22ml is needed. Given how difficult the sample is to make, and the resulting yields, this avenue was not explored further. The viscosity values are reported in Table 5-5. It is important to note that the viscosity values reported are not zero shear viscosity values, as no Newtonian plateau was observed.

Table 5-5. Viscosity values for NF395 taken at 0.1 s^{-1}

NF395	
Temperature (^{0}C)	Viscosity (Pa S)
20	54
25	36
30	25
35	18
40	13
45	10
50	8
55	6
60	5
65	4
70	3

5.2.6 NF1110

The following rotational method was developed to report the viscosity of NF1110. The selected geometry was a 15mm 2^0 cone along with the Peltier plate. The method consisted of shearing the sample from 0.1 s^{-1} to 3 s^{-1} for the temperatures of 20-70^{0}C. The measurements were conducted in 5^{0}C increments. A 10-minute equilibration period was given at each interval. Ten data points were taken per decade during the shear ramp. The results of the analysis are presented in Figure 5-22.

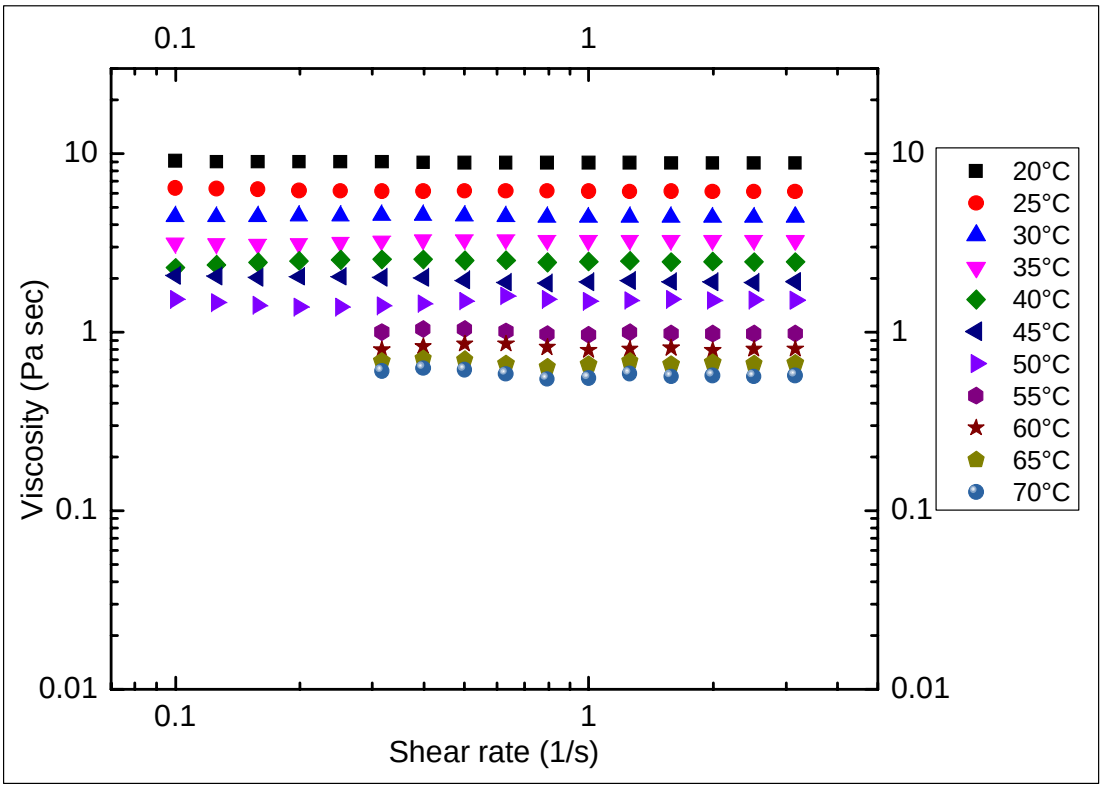

Figure 5-22. Flow curves for NF1110

This particular lot appeared to display Newtonian flow properties over the given shear range. Ideally, the sample would have been placed in the cuvette sample chamber. The viscosity values again indicated a very viscous type response. The numerical viscosity

values are shown in Table 5-6. It is important to note that the viscosity values reported are not zero shear viscosity values, as no Newtonian plateau was observed.

Table 5-6. Viscosity values for NF1110 taken at 0.1 s^{-1}

NF1110	
Temperature (^{0}C)	Viscosity (Pa S)
20	9
25	6.3
30	4.4
35	3.2
40	2.5
45	2
50	1.5
55	1.3
60	1
65	0.8
70	0.7

5.2.7 Discussion of Rotational Measurements

Examining the provided data can lead to the conclusion that increasing the amount of surface groups per nanoparticle results in solvent-free nanofluids of decreasing viscosity. The viscosity measurements conducted are relatively straightforward. Some difficultly was encountered with NF395 and NF1110, as no zero shear plateau was

detected. Even though no zero shear plateau was detected, the reported values were taken from very low shear rates and thus should be considered appropriate for comparison purposes. A summary of the varying SFN samples and their resulting viscosities are presented below in Table 5-7.

Table 5-7. Viscosity Comparison

Temperature ^{0}C	Viscosity (Pa S)					
	NF105	NF205	NF275	NF370	NF395	NF1110
30	555200	38800	19550	1314	25	4
50	51570	156	4277	207	8	2
70	1692	72	1221	57	3	0.7

The viscosity difference between NF370 and NF395 was extremely interesting. The analysis was repeated in triplicate with near identical results. However, when the samples were remade there were problems with reproducibility. The values reported above should not be considered "the viscosity" of solvent-free nanofluids with the respective surface groups per particle. However, the trend is clear; increasing the amount of ammonium groups per particle is a strategy for manipulating the viscosity of solvent free nanofluids.

Chapter 6

Coreless SFNs

Varying the shell thickness of solvent-free nanofluids discussed in Chapter 5 gave way to Professor John Texter's theory that core free nanofluids were possible. Two coreless solvent-free nanofluids were submitted for analysis. The manner in which they were prepared was similar to the Generation 1 nanofluids discussed above except it, obviously as the name suggests, did not utilize a nanoparticle core but used the strategy of auto-condensation.

6.1 Rheological Analysis of Coreless SFNs

The first coreless SFN generated was lot 08-1025-63P. This material was synthesized by Dr. Kejian Bian.

The general route for analyzing the rheology of Generation 1 SFNs was followed. The oscillation parameters for the temperature ramp are a frequency of 1 Hz and an initial oscillation torque of 10 μNm. An additional condition was added to the torque control. If the torque fell outside of the 0.5% tolerance, the instrument would revert to a 0.1% strain control. The temperature range chosen was 100 to -100^0C, with data points taken every 1^0C and a temperature ramp of 3^0C/minute. A second temperature ramp was conducted from -100 to 100^0C ,with data points taken every 0.5^0C and a temperature ramp of 3^0C/minute. The selected geometry was a 25mm parallel plate along with the environmental testing chamber. The results are shown in Figure 6-1.

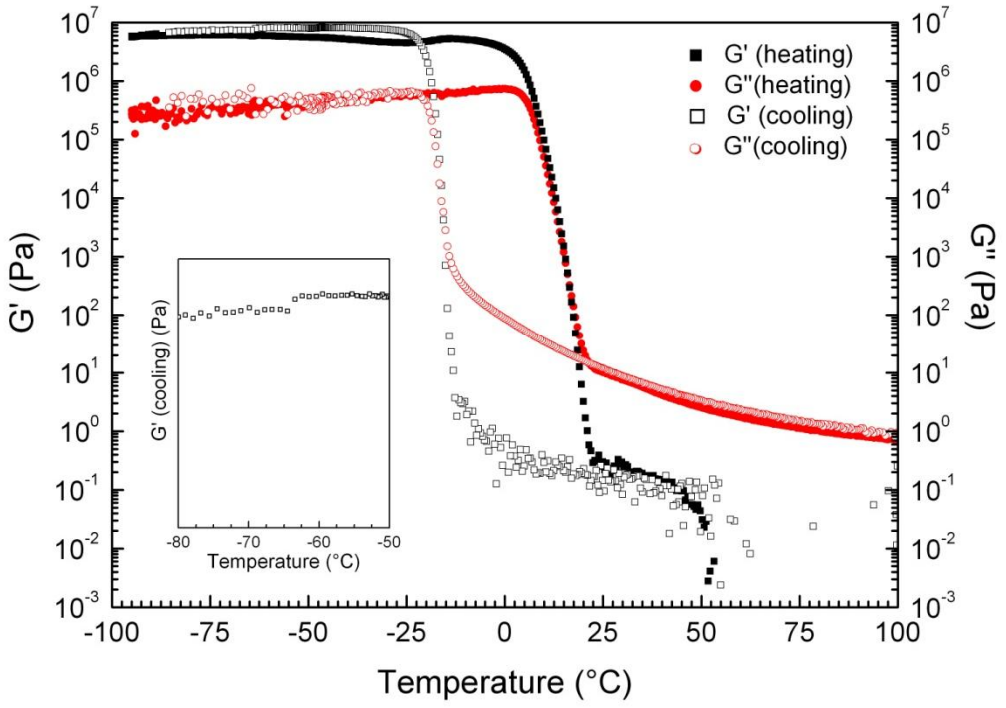

Figure 6-1. Temperature ramp for 08-1025-63P

The data clearly show the melting and solidification properties of the material. The solidification begins at approximately -13^{0}C and continues through -24^{0}C. The melting appears to take place at 3^{0}C and continues to approximately 25^{0}C. The reason for the hysteresis is unknown. Additionally, once again the Tg of the material was resolved at -64^{0}C. However, the Tg was only observed during the cooling cycle.

The following rotational method was developed to report the viscosity from the first Newtonian plateau. The selected geometry was a 15mm 2^0 cone along with the Peltier plate. The method consisted of shearing the sample from 0.1 s^{-1} to 2 s^{-1} for the temperatures of 30-70^{0}C. The measurements were conducted in 10^{0}C increments. A 10-minute equilibration period was given at each interval. Ten data points were taken per decade during the shear ramp. The results of the analysis are presented in Figure 6-2.

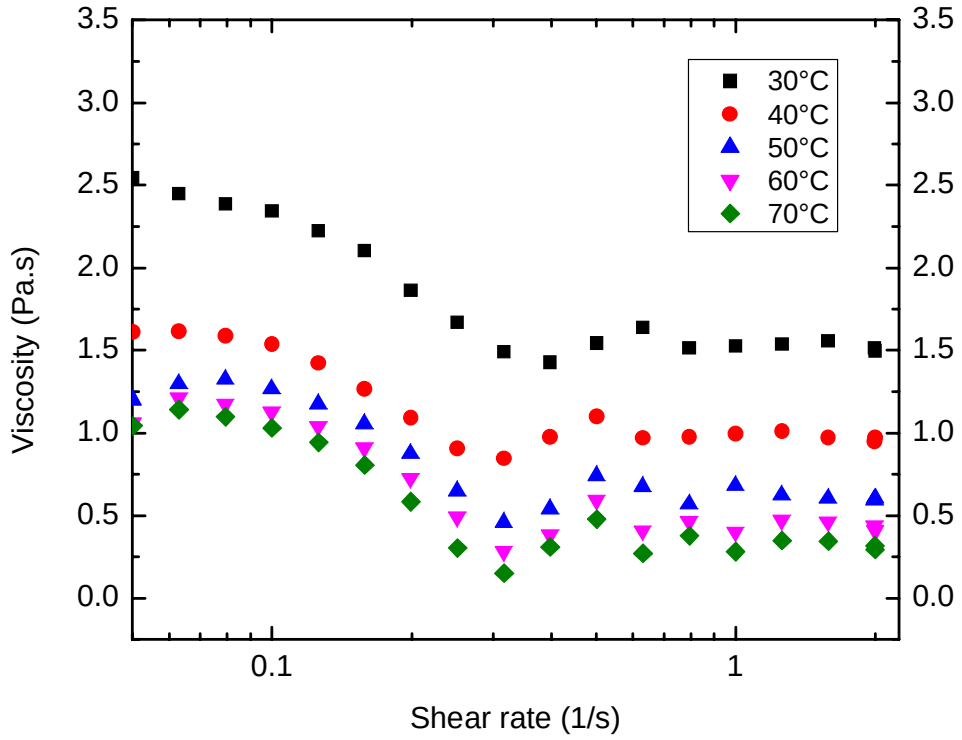

Figure 6-2. Flow curves for 08-1025-63P

The flow curves reveal an event around 0.05 to 0.3s^{-1}. In past experiments, some noise has been detected at low shear rates, but the data points were chaotic and not repeatable. The events between 0.05 to 0.3s^{-1}, however, were repeatable and appear to have a similar shape throughout the selected temperature range. In this instance, the viscosity will be reported from 1.0s^{-}, as it is unclear if the zero shear plateau exists. The numerical viscosity values are reported in Table 6-1.

Table 6-1. Viscosity values for lot 08-1025-63P taken from $1.0s^{-1}$

08-1025-63P	
Temperature (^{0}C)	Viscosity PaS
30	1.5
40	1
50	0.7
60	0.4
70	0.3

To gauge the repeatability of the coreless nanofluids, the sample was re-synthesized by Dr. Bian. The second lot submitted was identified as lot 08-1025-73. The initial thought process was to run a temperature ramp on the material, similar to the analysis run on 08-1025-63P. However, every time the temperature was lowered, the resulting increase in viscosity would dislodge the magnetic bearing, and the instrument would error out. This is thought to be due to a sudden change in viscosity and/or normal force. Different temperature ramps were utilized to attempt to resolve this problem, and the normal force control was even deactivated, but no success was obtained. No oscillatory data were generated for this lot.

Viscosity values were, however, taken, and the following rotational method was developed to report the viscosity from the first Newtonian plateau. The selected geometry was a 15mm 2^0 cone along with the Peltier plate. The method consisted of shearing the sample from 0.1 s^{-1} to 2 s^{-1} for the temperatures of 30-70^{0}C. The measurements were conducted in 10^0C increments. A 10-minute equilibration period was given at each

interval. Ten data points were taken per decade during the shear ramp. The results of the analysis are presented in Figure 6-3

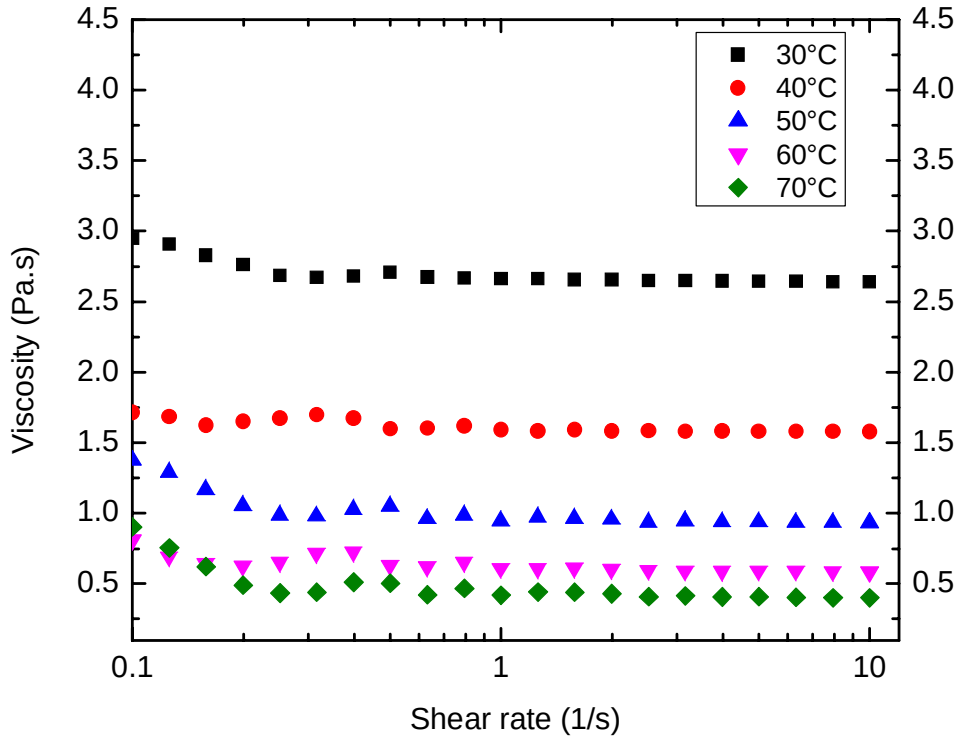

Figure 6-3. Flow curves for 08-1025-73

The flow curves again revealed some interesting noise-type behavior around $0.1s^{-1}$. In this case, these events did not appear to be repeatable. In this instance the viscosity will be reported from $1.0s^{-}$. In all the past measurements we've reported the viscosity from the zero shear plateau, but in this instance it is unclear if that plateau exists, and if it does, where the location of the plateau resides. The numerical viscosity values are reported in Table 6-2.

Table 6-2. Viscosity values of lot 08-1025-73 taken from $1.0s^{-1}$

08-1025-73	
Temperature (^{0}C)	Viscosity PaS
30	2.4
40	1.6
50	0.9
60	0.6
70	0.4

6.2 Discussion of Coreless SFNs Measurements

The rheology of the solvent-free nanofluids appeared to be relatively analogous to NF1110. The viscosity values obtained for both lots appeared to be relatively consistent with each other. However, it should be noted that the second batch (08-1025-73) may have been higher in viscosity, as it was the only sample to dislodge the magnetic bearing when it solidified. The unusual event at low shear rates is indeed noteworthy. Although the exact cause is not known, Dr. Texter hypothesized that it is the result of a high Mw component. The existence of the high molecular weight component was indeed confirmed during analytical ultra-centrifugation testing conducted at the Max Plank institute.

Chapter 7

Kenetic Study of Amino Substituted SFNs

7.1 Sample Preparation

Modifying the general SFNs synthesis to incorporate reactive functionality and then subsequently utilizing the reactive SFNs in coating formulations is an attractive avenue to alter the coatings properties and further develop the commercial prospects of SFNs.

An amine substituted SFNs material, lot 08-961-61, was synthesized at the Coatings Research Institute of Eastern Michigan University. The general reaction scheme is shown below in Figure 7-1.

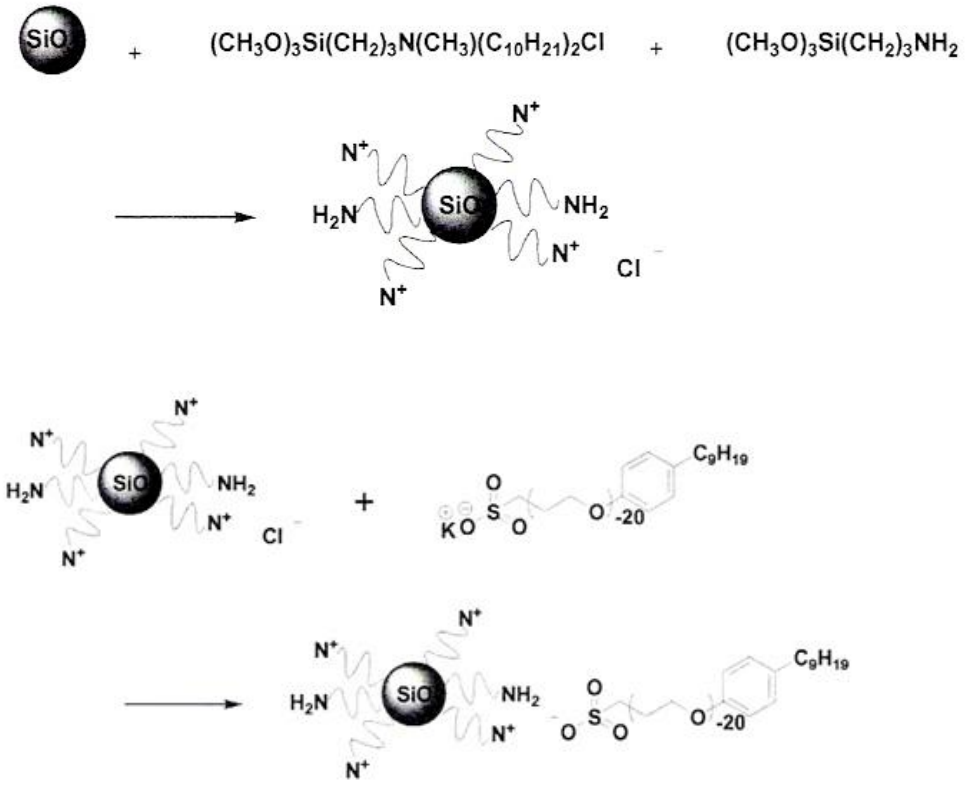

Figure 7-1. Synthesis of amine functional SFNs

Lot 08-961-61 had a Mn value of 586,000, and each SFNs molecule contained 100 reactive amine groups. The sample was submitted for a rheological cure analysis. The chosen counterpart for the SFNs to react with was propylene glycol diglycidyl ether (Mn 640). The chosen epoxy to amine ratio was 1.5. The experimental set up was such that the amine contribution would come from two sources. The first source was the SFNs, and the second was an auxiliary amine source. The auxiliary source was propylene glycol bis 2-aminopropyl ether (Mn 230). The amount of the SFNs was laddered in at 0%, 4%, 16%, and 32%. Due to the fact that the auxiliary amine component has a much lower equivalent weight, the amount of propylene glycol diglycidyl ether needed to be adjusted for each sample to ensure the stoichiometry was balanced. The amount of all three components in each sample can be viewed in Table 7-1.

Table 7-1: Sample preparation for cure analysis

SFNs weight percent of amine contributor	Amount of propylene glycol diglycidyl ether (g)	Amount of propylene glycol diaminopropyl ether (g)	Amount of SFNs lot 08-961-61 (g)	Epoxy : Amine ratio
0	1.5	0.36	0	1.5
4	4.01	0.96	0.04	1.5
16	3.52	0.84	0.16	1.5
32	2.86	0.68	0.32	1.5

7-2 Cure Study Utilizing Amino Functional SFNs lot 08-961-61

The experiment was conducted utilizing the 25mm parallel plate along with the environmental testing chamber. The test utilized to monitor the cure was the time sweep test. The chosen acquisition parameters was a frequency of 1Hz, temperature of 90^0C , normal force control activated at 0.0N with a 0.1N tolerance before gap adjustment, and the stress was applied via controlled strain at a rate of 0.1%. Controlling the stress via strain is a useful tool when large changes in viscosity are expected during the analysis. A sample rate of 1 point per ten minutes was collected.

The results of the analysis are displayed in Figure 7-2. The data indicate that incorporating the amine functional SFNs results in a slower cure. The effect becomes more dramatic when the weight percent of the SFNs increases in concentration. One hypothesis is that the reactive amine groups are buried beneath the ionic linkages, and thus their reactivity is decreased. Perhaps more significant than the cure delay are the final storage modulus values. The data indicate that the higher amount of amine functional SFNs present within the formulation, the softer the resulting film.

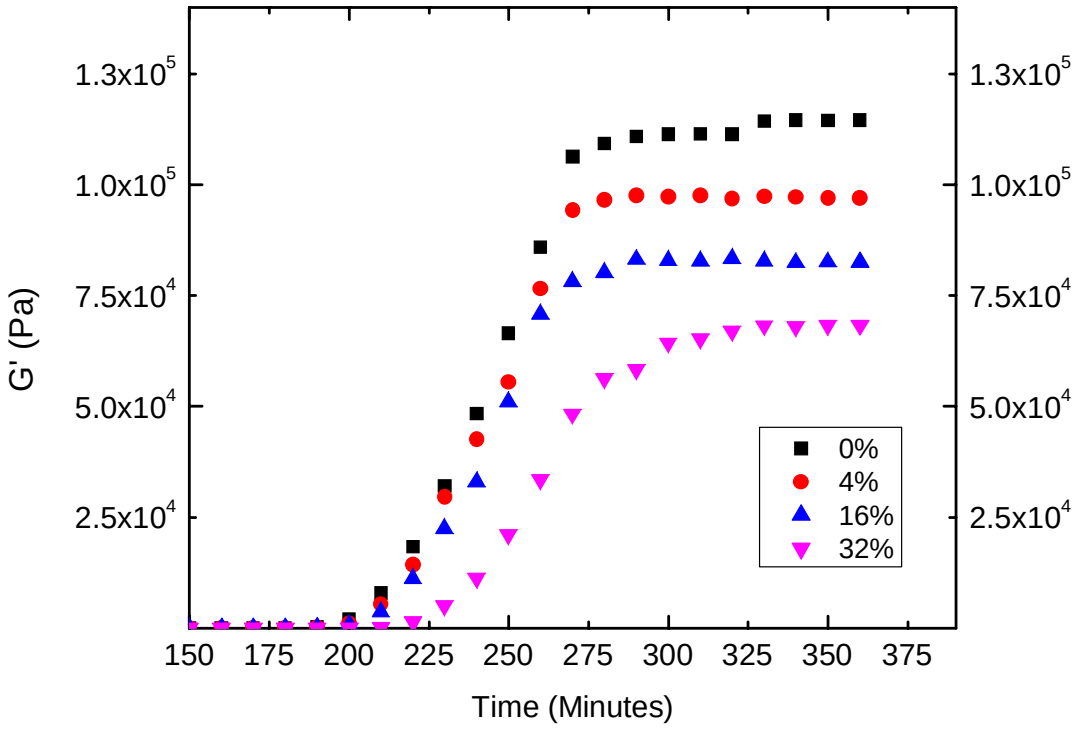

Figure 7-2. Time sweep of samples containing amine functional SFNs

Chapter 8: Viscosity of ionic liquid – Poly ($ILBF_4$)

A sample of Poly ($ILBF_4$) was synthesized and submitted for a viscosity analysis by Hong Gu. The following rotational method was developed to report the viscosity from the first Newtonian plateau. The selected geometry was a 25mm plate along with the Peltier plate inside the Environmental Testing Chamber. The method consisted of shearing the sample from 0.1 s^{-1} to 2 s^{-1} for the temperatures of 30-130^{0}C. The measurements were conducted in 10^{0}C increments. A 10-minute equilibration period was given at each interval. Ten data points were taken per decade during the shear ramp. The results of the analysis are presented in Figure 8-1.

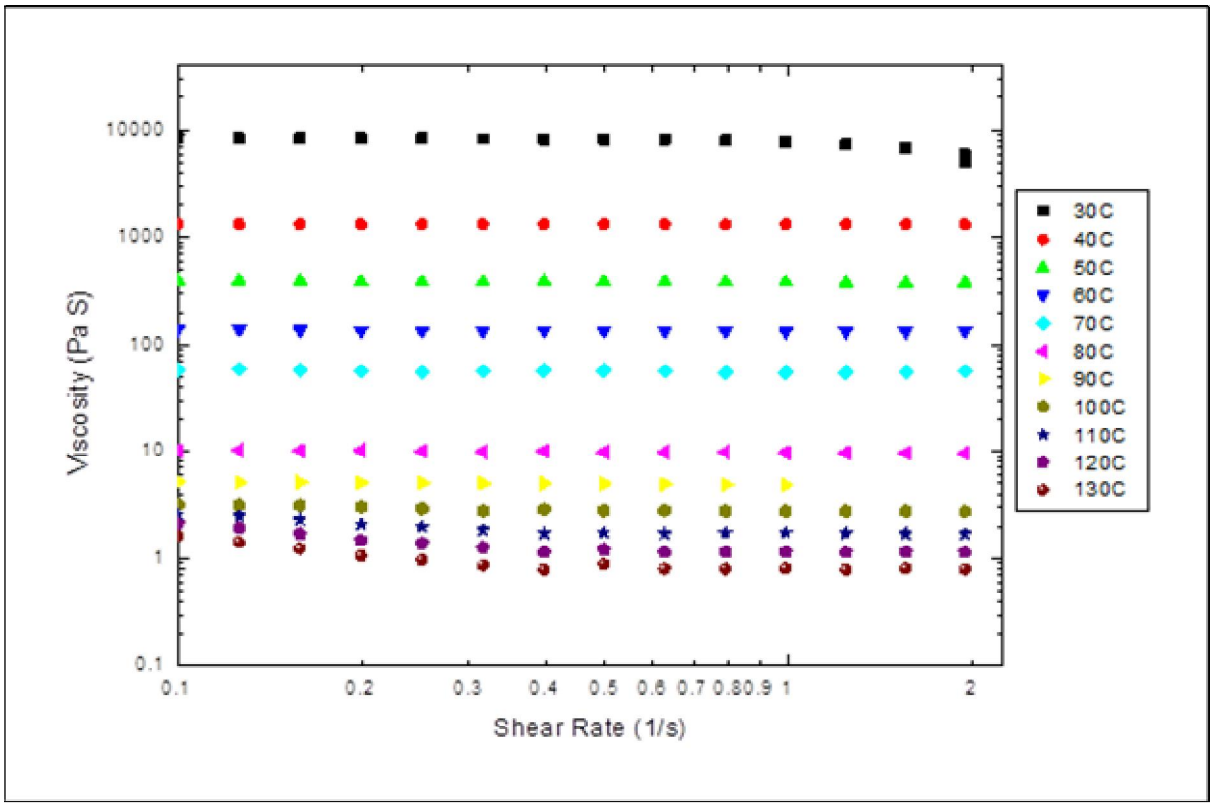

Figure 8-1. Flow curves of Poly ($ILBF_4$)

The resulting flow behavior appeared to be Newtonian at low shear rates. This flow behavior is particularly noteworthy as typically materials of this thickness ~10000 PaS at

30^0C tend to be very shear sensitive. The numerical viscosity values are report in Table 8-1

Table 8-1. Viscosity of Poly ($ILBF_4$)

Temp ^{o}C	30	40	50	60	70	80	90	100	110	120	130
Viscosity Pa. S	8356	1326	393	141	58	10	5.2	3.2	2.6	2.1	1.6

Chapter 9

Future works

The wide spectrum of flow behavior exhibited by the SNFs with varying shell thicknesses illustrates the importance of rheological support as a part of the research, development, and innovation of SFNs. Understanding and optimizing the rheology of SFNs is essential to tailoring them to their intended end use application. It is foreseeable that rheology could be utilized as an effective quality control procedure in SFNs production.

References:

1. Barnes, H. *A Hand Book of Elementary Rheology*; The University of Wales Institute of Non-Newtonian Fluid Mechanics: Department of Mathematics, University of Wales, 2000; pp 1-117.

2. Symon, K. *Mechanics;* Addison-Wesley: Massachusetts, 197; 295-345.

3. Meyers, A.A.; Chawla, K.K. *Mechanical Behavior of Materials*; Cambridge University Press: New York, 2009; pp 98-103.

4. Franck, A. J. TA Instruments . http://www.tainstruments.com/maiNaspx?n=2&id=181&main_id=177&siteid=11 (accessed Aug 17, 2008),), Understanding the Rheology of Structured Fluids.

5. Franck, A. J. TA Instruments. http://www.tainstruments.com/maiNaspx?n=2&id=181&main_id=174&siteid=11 (accessed Aug 17, 2008), Understanding the Rheology of Thermoplastic Polymers.

6. Bohnsak, D.; Rheology - AR Series Theory and Application Course. Presented at TA Instruments Rheology Theory and Applications Training Course, New Castle DE, Aug 5-8, 2007.

7. Franck, A. J. TA Instruments . http://www.tainstruments.com/maiNaspx?n=2&id=181&main_id=115&siteid=11 (accessed Aug 17, 2008), Application Rheology of Polymers.

8. Marrucci, G.; Greco, F.; Ianniruberto, G. Rheology of Polymer Melts and Concentrated Solutions. *Curr. OpiN Colloid Interface Sci.* **1999**, 4, 283-287.

9. Franck, A. J. TA Instruments . http://www.tainstruments.com/maiNaspx?n=2&id=181&main_id=175&siteid=11

(accessed Aug 17, 2008),), Understanding the Rheology of Thermosetting Polymers.

10. Goh, T.; Coventry, K.; Belcowe, A.; Qjao, G. Rheology of Core Cross-Linked Star Polymers. *Polymer*. **2008**, 49, 5095-5104.

11. Bergenholtz, J. Theory of Rheology of Colloidal Dispersions. *Curr. OpiN Colloid Interface Sci*. **2001**, 6, 484-488.

12. Tanner, R. The Changing Face of Rheology. *J. Non-Newtonian Fluid Mech.* **2009**, 157, 141-144.

13. Boger, D. Rheology and the Resource Industries. *Chem. Eng. Sci.***2009**, 64, 4525-4536.

14. Derkach, S. Rheology of Emulsions. *Adv. Colloid Interface Sci.***2009**, 151, 1-23.

15. Puyvelde, P.; Velankar, S.; Moldenaers, P. Rheology and Morphology of Compatibilized Polymer Blends. *Curr. OpiN Colloid Interface Sci.* **2001**, 6, 457-463.

16. Rodrigues, R.; Herrera, R.; Archer, L.; Giannelis, E. Nanoscale Ionic Materials. *Adv. Matter*. **2008**, 20, 4353-4358.

17. Xiong, H.; Shen, W.; Wang, Z.; Zhang, X.; Xia, Y. Liquid Polymer Nanocoposites PEGME-SnO_2 and PEGME-TiO_2 Prepared through Solvothermal Methods. *Chem Matter*. **2006**, 18, 3850-3854.

18. Warren, S.; Banholzer, M.; Slaughter, L.; Giannelis, E.; DiSalvo, F.; Wiesner, U. Generalized Route to Metal Nanoparticles with Liquid Behavior. *J. AM. Chem. Soc.* **2006**, 128, 12074-12075

19. Bourlinos, A.; Herrera, Chalkias.; Jiang, D.; Zhang, Q.; Archer, L.; Giannelis, E. Surface Functionalized Nanoparticles with Liquid like Behavior. *Adv. Mater.* **2005**, 17, 234-237.

20. Bourlinos, A.; Giannelis, E.; Zhang, Q.; Archer, L.; Floudas, G.; Fytas, G. Surface Functionalized Nanoparticles with Liquid like Behavior: The role of the Constituent Components. *Eur. Phys. J. E.* **2006**, 20, 109-117.

21. Berthoods, A.; Carda-Broch, S. Downloaded on Oct. 25th, 2008 from http://www.mariecurie.org/annals/volume3/berthod.pdf

22. Fernicola, A.; Scrosati, B.; Ohno, H. *Ionics* **2006,** *12*, 95-102.

23. Wasserscheid, P.; Keim, W. *Angew. Chem. Int. Ed.* **2000**, *39*, 3772-3789.

24. Earle, M. J.; Seddon, K. R.; *Pure Appl. Chem.* **2000**, *72(7)*, 1391-1398.

Appendix 1:
Operating Instruction for the AR-G2

1.0 SCOPE:

This method is applicable for general operation of the AR-G2 Rheometer to determine rheological characteristics.

2.0 APPLICATION:

This instruction applies to all students using the AR-G2 Rheometer.

3.0 PERSONAL SAFETY EQUIPMENT:

Safety glasses, protective gloves, protective clothing

4.0 ASSOCIATED MATERIALS:

TA Instruments AR-G2 Rheometer

Up to 25mL of sample - depending on the geometry to be used

Appropriate geometry (standard DIN, cone and plate, parallel plate)

5.0 ROUTINE:

A. Start-Up Procedure

5.01 Make sure there is 30 ± 2psi of pressure being regulated to the rheometer. If not, adjust regulator until there is proper air pressure or consult the analytical manager.

5.02 Check to see if the black air bearing cap (which is black and screws into the same locations the geometries do) is in place. If it is - **REMOVE THE AIR BEARING LOCK FROM THE RHEOMETER!!** This must be done first to ensure that the air bearing is not broken during start-up.

5.03 Turn on the computer for the AR-G2 and open the software by the "AR Instrument Control" icon on the desktop.

B. General Setup

5.04 Screw in the geometry to be used.

5.05 If using the DIN, the concentric cylinder needs to be in place. If using the cone and plate or parallel plate, the Peltier plate needs to be in place. To change the plates, hit the  "Release Button" on the front of the instrument. The green light will flash, indicating that it is safe to disconnect the attachment.

5.06 Hit the "Release Button" a second time to display a continuous green light, indicating that you can remove the plate. Disconnect both fluid cables and remove plate.

5.07 When the green light goes out, hit the "Release Button" again to get a continuous green light, indicating that a plate can be added, connect the attachment. Connect both fluid cables.

5.08 On the main menu of the software there are 5 main buttons. Hit the first button see the Instrument Status. Here, an operator can maintain control over basic instrument functions.

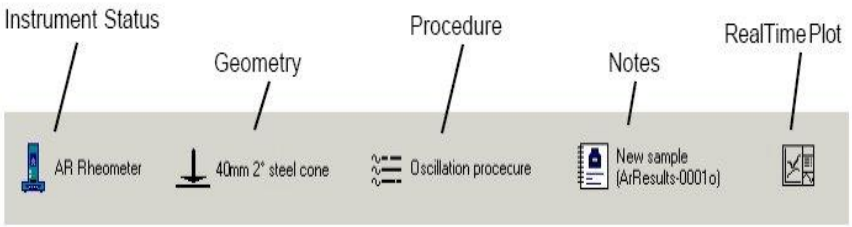

5.09 Once the proper plate is in place, on the instrument status screen set the temperature to 25°C by double clicking on temperature. Hit 'Enter' to send the data and close the window.

5.10 Slide the geometry onto the draw rod and holding it still, turn the top of the rod clockwise to tighten the two together. Snug the rod tight, DO NOT OVER TIGHTEN.

5.11 The geometry will automatically be recognized with the Smart Swap technology and will begin to rotate as the software sets up. When the software is ready, it will ask to perform Rotational Mapping, say 'NO' at this time.

5.12 Spin the top of the draw rod to get the geometry moving – take note of the geometry in motion.

5.13 Hit the  "Head Down" button, until the geometry is within 5mm of the bottom of the concentric cylinder or Peltier plate and slow down the head.

5.14 Hit the  "Zero Gap" Button and allow the instrument to automatically set the gap for the geometry

5.15 When the gap is set, it will prompt to raise the head to the back-off distance.

5.16 Click "Yes".

5.17 Hit the  "Rotational Mapping" button to perform the mapping of the optical encoder. The settings need to be 'Precision' and '1'. It will take about 5 minutes to perform and should be completed every day.

C. Sample Fill for Concentric Cylinder

5.18 Using a transfer pipette, add approximately 10 pipettes of sample (~19.6mL of sample) to the concentric cylinder, adjusting the amount of sample based on the viscosity.

5.19 Add the bottom of the solvent trap (with the moat) to the top of the concentric cylinder and fill with a solvent that is compatible with the paint sample.

5.20 On the instrument status screen, double click on the 'Shear Rate', enter 100 (1/s) and hit 'Enter'.

5.21 The geometry will begin to rotate.

5.22 Hit the button to  lower the head to the proper geometry gap. The rotating geometry will help to eliminate any air bubbles that may be trapped in the sample .

5.23 Once the geometry is at the gap position, if necessary, continue to fill the concentric cylinder with sample until it is approximately 2-

3mm from the top of the cylinder (NOT the solvent trap). Thin samples should be filled to the lower level to prevent loss during high shear.

5.24 Place both halves of the top of the solvent trap in place

D. Sample Fill for Cone and Plate and Parallel Plates

5.25 For the cone, add approximately 1.5 mL to the center of the Peltier plate with a transfer pipette.

5.26 On the instrument status screen, double click on the 'Shear Rate', enter 100 (1/s) and hit 'Enter'.

5.27 The geometry will begin to rotate.

5.28 Hit the button to  lower the head to the proper geometry gap. The rotating geometry will help to even out the sample under the geometry.

5.29 Cleanly wipe off excess sample (also called trimming) or add additional sample by using a transfer pipette at the edge of the rotating geometry. Additional sample will be pulled under the geometry. There is just enough sample when it comes in contact with, but does not appear to be bowing inward or outward from the edge of the geometry.

E. Data Collection and Data Analysis – Obtaining Graphs

5.30 On the main menu of the software, hit the 3rd button for Procedure. Hit the 'Open' button and select the procedure to be used (listed by product).

5.31 On the main menu of the software, hit the 4th button for the Notes. Hit the 'Open' button and select the corresponding notes file (listed by product).

5.32 When ready, hit the  Green Arrow to "Run Experiment".

5.33 The ‘Run Experiment Information’ window will open. Enter the charge number if relevant and any important details in the Experimental Notes section of the Notes file such as trial or test data. A unique Notes file can be saved with each individual sample so detailed information can be collected and recorded.

5.34 Click ‘OK’. The test will begin automatically.

5.35 On the main menu of the software, the 5th button for ‘Real Time Plot’ will be accessed automatically. You can watch the testing running in real time and monitor when the testing is complete.

5.36 When testing is complete, hit the  “Analyze Results” button.

5.37 If the filename does not appear in the left column, hit the  “Refresh” Button and it should appear. Double click on the filename and all data will appear on the graph to the right.

5.38 In the graph, right-click and select ‘Miscellaneous’

5.39 Under the ‘Steps Displayed’, select or de-select the steps for the test results you’d like to review.